Interpretation of in-situ gas experiment PGZ1

FORGE Report D5.9 - VER.0

	Name	Organisation	Signature	Date
Compiled	Rémi de La Vaissière	ANDRA		06/12/2011
Verified	Jean Talandier	ANDRA		
Approved	RP Shaw	BGS		

Keywords

argillite, Callovo-oxfordian, gas migration, gas entry pressure.

Bibliographical reference

de La Vaissière, Rémi. 2011. Interpretation of in-situ gas experiment PGZ1. FORGE Report D5.9 70pp.

Euratom 7th Framework Programme Project: FORGE

Fate of repository gases (FORGE)

The multiple barrier concept is the cornerstone of all proposed schemes for underground disposal of radioactive wastes. The concept invokes a series of barriers, both engineered and natural, between the waste and the surface. Achieving this concept is the primary objective of all disposal programmes, from site appraisal and characterisation to repository design and construction. However, the performance of the repository as a whole (waste, buffer, engineering disturbed zone, host rock), and in particular its gas transport properties, are still poorly understood. Issues still to be adequately examined that relate to understanding basic processes include: dilational versus visco-capillary flow mechanisms; long-term integrity of seals, in particular gas flow along contacts; role of the EDZ as a conduit for preferential flow; laboratory to field up-scaling. Understanding gas generation and migration is thus vital in the quantitative assessment of repositories and is the focus of the research in this integrated, multi-disciplinary project. The FORGE project is a pan-European project with links to international radioactive waste management organisations, regulators and academia, specifically designed to tackle the key research issues associated with the generation and movement of repository gasses. Of particular importance are the long-term performance of bentonite buffers, plastic clays, indurated mudrocks and crystalline formations. Further experimental data are required to reduce uncertainty relating to the quantitative treatment of gas in performance assessment. FORGE will address these issues through a series of laboratory and field-scale experiments, including the development of new methods for up-scaling allowing the optimisation of concepts through detailed scenario analysis. The FORGE partners are committed to training and CPD through a broad portfolio of training opportunities and initiatives which form a significant part of the project.

Further details on the FORGE project and its outcomes can be accessed at www.FORGEproject.org.

Contact details:

de La Vaissière, Rémi
ANDRA
Tel: 33 (0) 329 755 343 Fax 33 (0) 637 262 539
email: remi.delavaissiere@andra.fr
web address: www.andra.fr
Address **Laboratoire de recherche souterrain de Meuse / Haute-Marne**
Route départementale 960
BP 9
55290 Bure FRANCE

FOREWORD

This report is the second ANDRA report concerning the PGZ1 experiment since the equipment was first installed in the French URL. It follows report "design and installation of the PGZ1 experiment at Bure" (deliverable D5.4), which describes the objectives of the PGZ experiment, the experimental setup for PGZ1 and the initial results obtained by mid-November 2009.
This report combines the deliverables D5.9 and D5.12 of the FORGE project.
For modellers, all data measurements are available on request (remi.delavaissiere@andra.fr).

ACKNOWLEDGEMENTS

The research leading to these results has received funding from the European Atomic Energy Community's Seventh Framework Programme (FP7/2007-2011) under Grant Agreement n°230357, the FORGE project

CONTENTS

Foreword 3

Acknowledgements 3

Contents 4

1. Summary 7

2. Introduction 7

3. General description of the PGZ1 test 8

3.1 Overview of the experimental setup of the PGZ1 test 8

3.2 History 12

3.3 Presentation of the measurements over the whole test period 14

4. Period prior to the gas injection phase 20

4.1 Hydraulic tests in Interval 2 of PGZ1201 20

4.2 Interstitial-pressure measurements (PGZ1201 & PGZ1202) 21

4.3 Pressure measurements for the (PGZ1201) packers 23

4.4 Convergence phenomena 24

5. Gas-water exchange phase 25

5.1 Measurements 25

5.2 Volume of Interval 2 27

5.3 Pressure variation 28

6. Rising gas pressure phases 30

6.1 Measurements 31

6.2 GRIx injection steps 34

6.3 Comparison of the GRISx pressure recovery steps 39

7. Gas extraction and water refilling phase 41

7.1 Pressure measurements 41

7.2 Hypothesis concerning packer behaviour 43

7.3 Gas extraction phase (GRE) 46

7.4 Refilling with water 49

8. Summary 51

8.1 Main results 51

8.2 Comparaison between HYDRO2 versus HYDRO1 53

Appendix 1 Gas module 54

Appendix 2 Sensor datasheets for the three gas flowmeters 55

PGZ1201DGZ01 55

PGZ1201DGZ02 57

PGZ1201DGZ03 59

Appendix 3 Volume for the gas module and extraction system 61

Appendix 4 Mass balance 62

9. Glossary 63

10. References 63

FIGURES

Figure 1 Phenomenological description of gas transport processes in argillaceous rock (Marschall et al., 2005) 7
Figure 2 Borehole positions for test PGZ1 9
Figure 3 Detailed geometry around the gas injection interval (PGZ1201PRE02) 10
Figure 4 Standard schematic diagram of an interval in a 76-mm-diameter borehole 11
Figure 5 Standard schematic diagram of a borehole-end interval in a 76-mm-diameter borehole 11
Figure 6 Pressure measurements for the three intervals and two packers of PGZ1201 over the whole test period 14
Figure 7 Pressure measurements for the three intervals of PGZ1202 over the whole test period 15
Figure 8 Anchor positions for borehole PGZ1031 17
Figure 9 Monitoring of relative displacement measurements for PGZ1031 (t_0 = installation) over the whole period 18
Figure 10 Monitoring of relative displacement measurements for PGZ1031 (t_0 = 1 August 2009) over the whole test period 19
Figure 11 Relative discrepancies between two consecutive anchorages (t_0 = 1 August 2009) over the whole test period; positive discrepancy = elongation 19
Figure 12 Observed and simulated hydraulic interference for the constant pressure test 21
Figure 13 Measurements of PGZ1201 and PGZ1202 interstitial pressure between July 2009 and February 2010 22
Figure 14 Simulation of the changes in pressure at various distances from PGZ1031 for a drainage taken as equivalent to a constant pressure boundary equal to atmospheric pressure 23
Figure 15 Pressure measurements for the packers surrounding Interval 2 of PGZ1201 and pressure measurement at Interval 2 between July 2009 and February 2010 24
Figure 16 Measurements of water and gas pressure during the water-gas exchange phase for Interval 2 of PGZ1201 (28 January 2010) 26
Figure 17 Monitoring gas pressure and flowrate from 28 January 2010 to 1 February 2010 27
Figure 18 Schematic drawing of the various volumes that make up Interval 2 of PGZ1201 28
Figure 19 Pressure variations as measured and as calculated for constant volume for injection at constant pressure 29

Figure 20	Pressure and gas flowrate measurements in PGZ1201 from January 2010 to April 2011	31
Figure 21	Detail of the pressure measurements for Intervals 1 and 3 of PGZ1201 from January 2010 to April 2011	32
Figure 22	Pressure measurements in PGZ1202 from January 2010 to April 2011	32
Figure 23	Comparison of the packer pressure measurements and gas-injection interval pressure (PGZ1201) from January 2010 and April 2011	34
Figure 24	Flowrate and cumulative quantity of gas injected and pressure measured in Interval 2 of PGZ1201 during GAS1	35
Figure 25	Pressure difference measured for the six injection steps GRI1 to GRI6 adjusted for a normalised gas flowrate of 1 ml_n/min	36
Figure 26	Comparison of the pressure difference as measured and as calculated at constant volume for the six steps GRI1 to GRI6	37
Figure 27	Pressure discrepancies calculated without the gas compressibility effect, normalised to an injection flowrate of 1 ml_n/min	39
Figure 28	Pressure difference measured during the pressure recovery steps (GRIS1 to GRIS6)	40
Figure 29	Horner plot for the GRISx steps	41
Figure 30	Pressure measurements for the three intervals and two packers of PGZ1201 during the extraction phase and after refilling with water	42
Figure 31	Pressure measurements for the three intervals of PGZ1202 during the extraction phase and after refilling with water	42
Figure 32	Comparison of the packer pressure measurements and gas-injection interval pressure (PGZ1201) from January 2010 and April 2011	44
Figure 33	Propagation of the overpressure along a packer during a pressure recovery phase	44
Figure 34	Monitoring interstitial pressure (red, green) and pressure in PGZ1013 packers (blue, khaki)	45
Figure 35	Specific storage as a function of saturation	46
Figure 36	Schematic diagram of the extraction system	47
Figure 37	Flowrate and cumulative quantity of gas extracted, and pressure measured in Interval 2 of PGZ1201 during the GRE phase	48
Figure 38	Comparison of the pressure difference as measured and as calculated at constant volume for the extraction phase	49
Figure 39	Pressure measurements PGZ1201PRE02 and PGZ1201PGZ01 recorded on 5 May 2011 from midday to 8pm	50
Figure 40	Calculated pressure variation for all injection and pressure recovery steps	53
Figure 41	Photograph and schematic diagram of the gas module	54

TABLES

Table 1	Shortest wall-to-wall 3D distances between the measurement intervals and borehole PGZ1031	10
Table 2	Simplified PGZ1 logbook	12
Table 3	Pressure-reduction gradients observed in PGZ1201 for two dates	15
Table 4	Pressure-reduction gradients observed in PGZ1202 for two dates	16
Table 5	Parameters for the rock around Interval 2 of PGZ1201 (HYDRO1)	20
Table 6	Variations in the volume and diameter of packers PPK01 and PPK02 between 24 August and 18 January	24
Table 7	Summary of the GRIx and GRISx rising pressure steps	30
Table 8	Results of HYDRO2 and HYDRO1	51
Table 9	Compressibility values for Intervals 1 and 3 of PGZ1201 and Intervals 1 to 3 of PGZ1202 measured on 2 August 2011	51
Table 10	Mass balance between gas injection and extraction	62

1. Summary

This report describes something that we did as part of the FORGE research programme…
The first part of the report introduces the project and the context of this particular bit of work.
Etc., etc.

2. Introduction

This report is the second ANDRA report concerning the PGZ1 experiment since the equipment was first installed in the "experimental drift two (GED)" Programme Unit. It follows report "design and installation of the PGZ1 experiment at Bure" (deliverable D5.4), which describes the objectives of the PGZ experiment, the experimental setup for PGZ1 and the initial results obtained by mid-November 2009. **This report combines the deliverables D5.9 and D5.12 of the FORGE project.**

The purpose of the PGZ1 test is to characterise the properties of gas transfer through the formation. This involves validating or improving the parameters and limits of the standard two-phase model used to represent gas transfer:

- Determining the entry pressure of the gas into undisturbed argillite and, if possible, into the excavated damaged zone (EDZ),
- Determining the gas pressure threshold beyond which pathway dilation may occur in the argillite,
- Determining how this threshold relates to the fracture pressure,
- Characterising the network of microcracks (pathway dilation) created (reversible or otherwise).

The current conceptual model adopted for the argillites has four transfer modes which depend on the gas production dynamics, the formation's pore structure and the stresses on the formation.
The various transfer mechanisms are summarised in Figure 1.

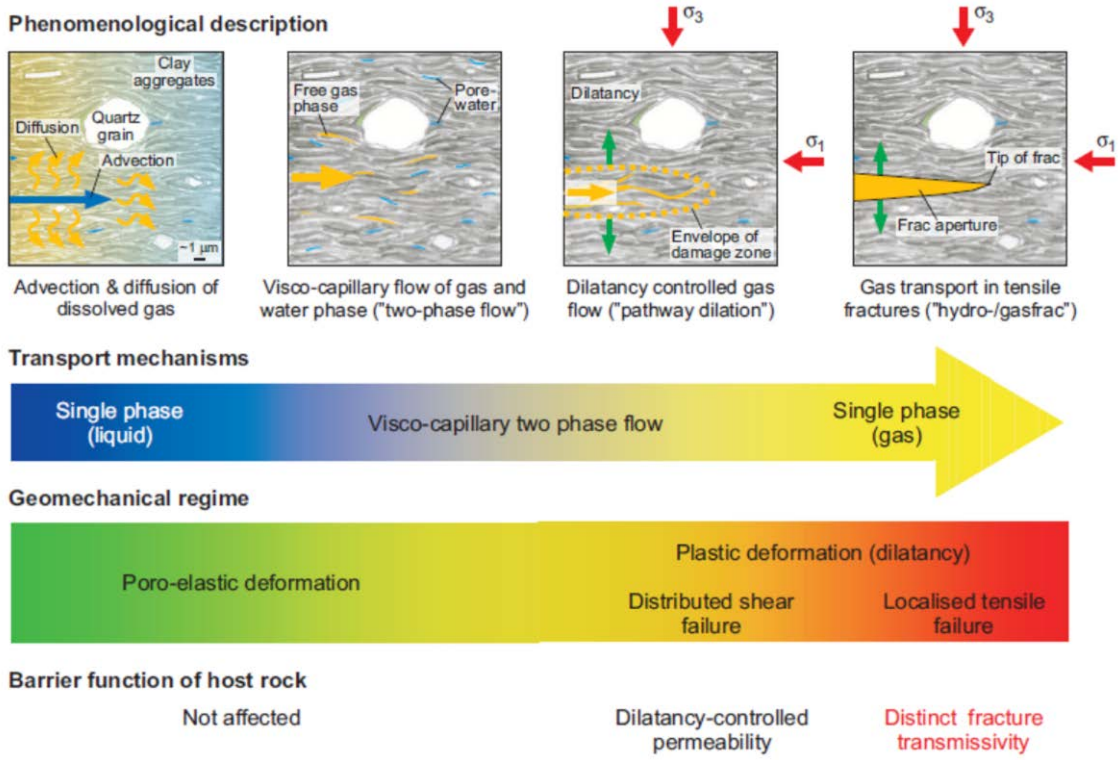

Figure 1 *Phenomenological description of gas transport processes in argillaceous rock (Marschall et al., 2005)*

1. The initial gas transfer mode corresponds to the removal of dissolved gas via convection or diffusion.
2. The second transfer mode appears, below the pathway dilation threshold, after local flow paths open. In this mode, gas permeability does not change as a function of gas pressure but the relative permeability of the gas changes as a function of saturation.
3. The third transfer mode assumes the appearance of pathway dilation beyond a certain gas pressure. The permeability of the gas is expected to increase as the gas pressure increases (hydro-mechanical coupling). Questions remain as to whether this transfer mode exists for argillite.
4. The final transfer mode corresponds to rock fracture after the gas pressure has exceeded the minimum stress. This transfer mode has already been demonstrated in argillite during the deep borehole gas injection test EST363 (D.RP.0GOL.05.001 "Gas threshold pressure test – interpretation report – borehole EST363").

The main purpose of the PGZ1 test is to understand and quantify the behaviour of gas in undamaged rock below the fracture pressure. This involves determining the pressure threshold for gas entry and the pressure threshold beyond which pathway dilation may occur.
For this, an initial gas injection phase was performed between February 2010 and May 2011. This first phase, called "GAS1", was comprised of a series of constant-flowrate gas injections (injection steps) separated by pauses during which the pressure was monitored (pressure recovery steps).
This report gives all the measurements taken during test PGZ1 up to the beginning of August 2011 and offers a detailed analysis of the GAS1 phase. It is structured according to the chronology of the steps, with a period prior to gas injection, the gas-water exchange phase, the rising gas pressure phase, the gas extraction phase and the refilling of the interval with water. The section that describes the pressure rise phase is both the most important and the longest.
All data measurements are available on request (remi.delavaissiere@andra.fr).

3. General description of the PGZ1 test

3.1 Overview of the experimental setup of the PGZ1 test

A brief summary of the PGZ1 test configuration is given below, to make it easier to follow the later sections. For more details, please refer to "design and installation of the PGZ1 experiment at Bure" (deliverable D5.4).

3.1.1 Layout

The boreholes for test PGZ1 are positioned as shown in Figure 2.

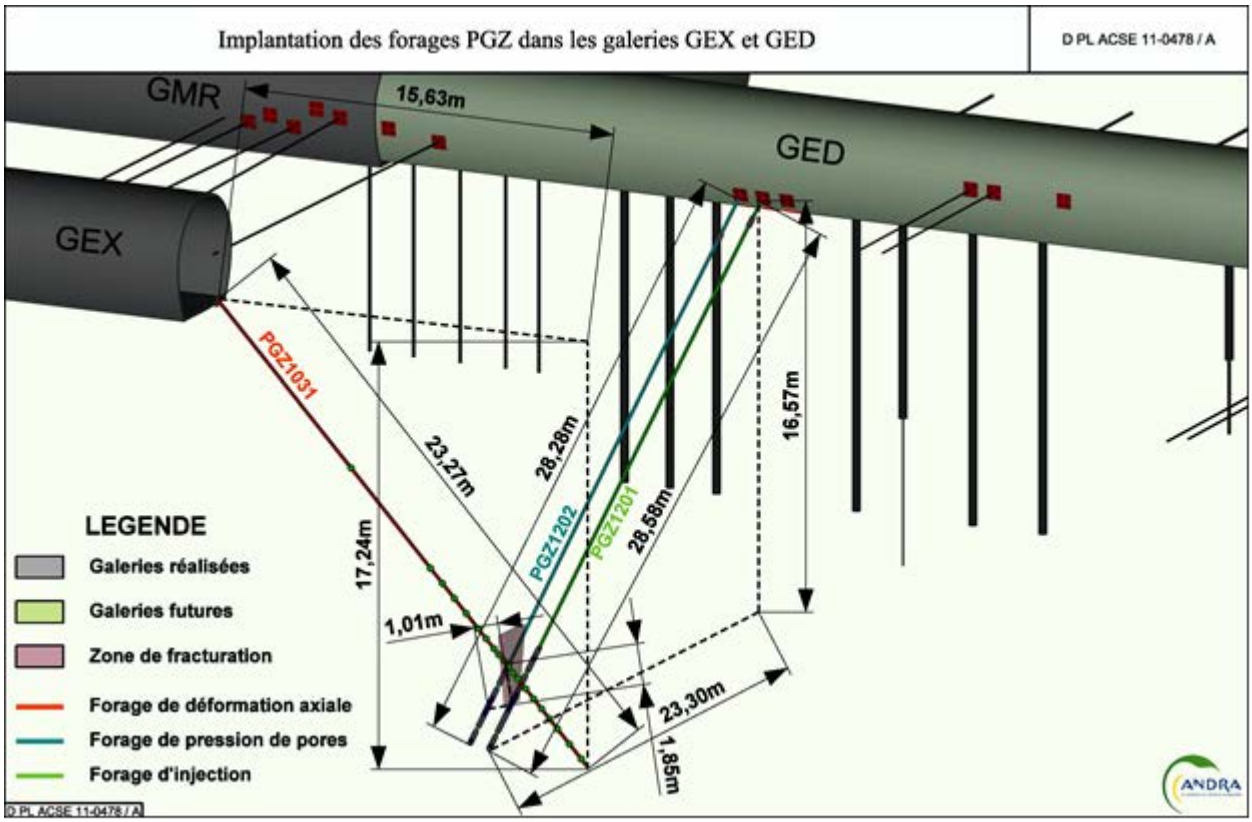

Figure 2 Borehole positions for test PGZ1

Boreholes PGZ1201 and PGZ1202 run parallel. Both are fitted with multi-packer systems with three interstitial-pressure measurement intervals. Borehole PGZ1031 passes above boreholes PGZ1201 and PGZ1202 and is fitted with rings for measuring displacements in the borehole axis. All three boreholes have a descending incline.

Borehole PGZ1201 is used to inject gas into the formation's interval. The injection interval's reference number in the SAGD (data acquisition and management system) is PGZ1201PRE02.

The distances between intervals are shown in Figure 3, along with the components of the SAGD reference numbers for the measurement points.

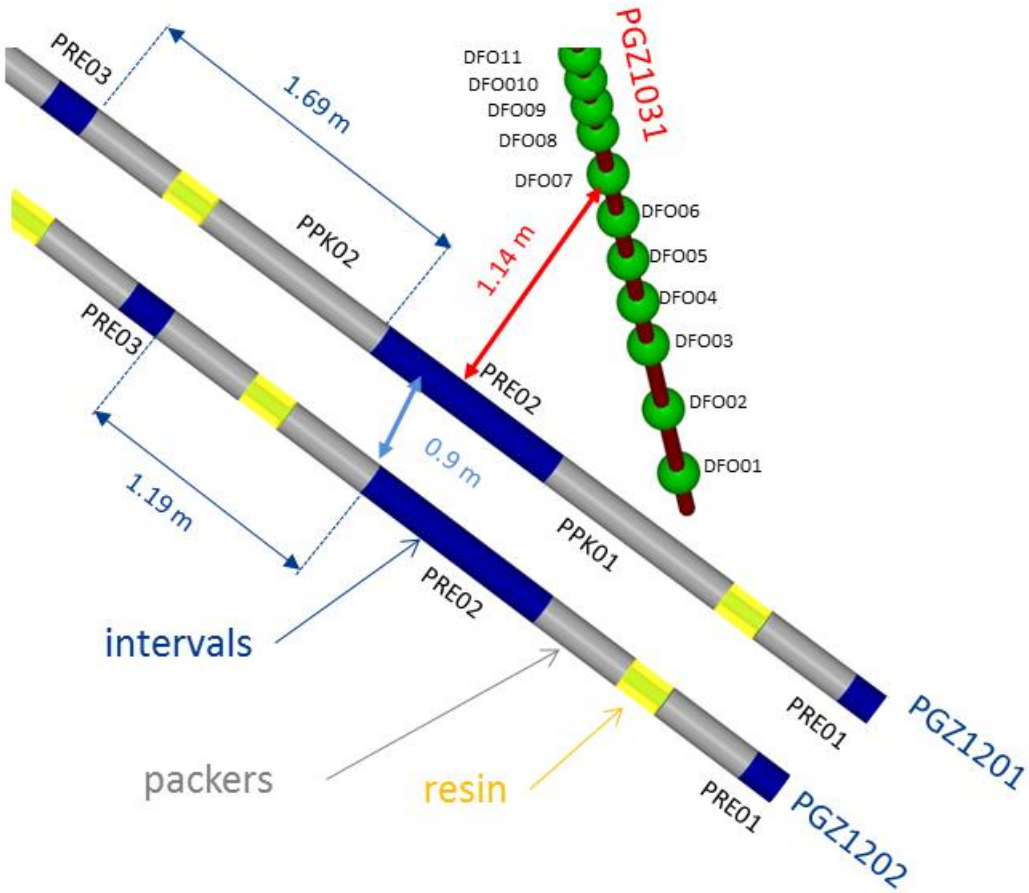

Figure 3 *Detailed geometry around the gas injection interval (PGZ1201PRE02)*

The (shortest wall-to-wall) 3D distances between the six interstitial-pressure measurement intervals and borehole PGZ1031 are given in Table 1.

Table 1 *Shortest wall-to-wall 3D distances between the measurement intervals and borehole PGZ1031*

	Interval 1	**Interval 2**	**Interval 3**
PGZ1201	2.31 m	1.14 m	2.20 m
PGZ1202	2.74 m	1.90 m	2.15 m

3.1.2 Equipment characteristics

3.1.2.1 Measurement intervals

All the intervals are 200 mm long, except for Interval 2 on both PGZ1201 and PGZ1202 which are 1 m long.

The interval comprises a stainless steel inner pipe (42 mm internal diameter, 65 mm external diameter) surrounded by a 2-mm-thick stainless steel filter with a porosity of 30% (internal diameter 66 mm, external diameter 70 mm). Two stainless steel lines (2.4 mm and 4 mm) are placed in each interval. Standard schematic diagrams of the intervals are shown in Figure 4 and Figure 5.

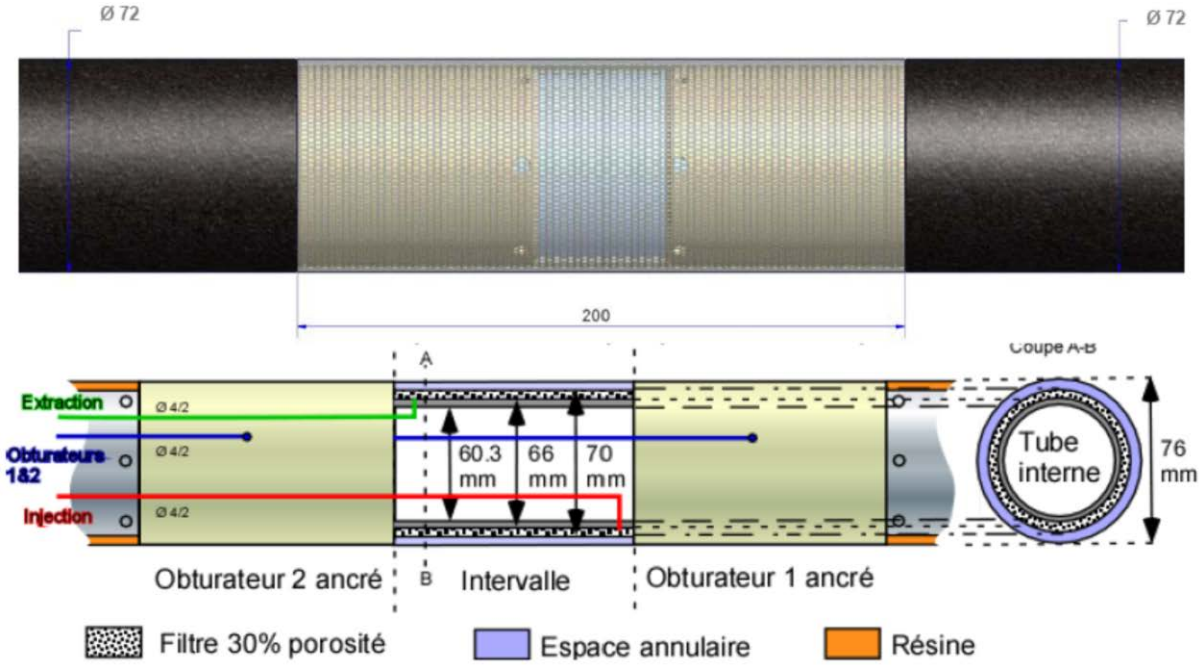

Figure 4 *Standard schematic diagram of an interval in a 76-mm-diameter borehole*

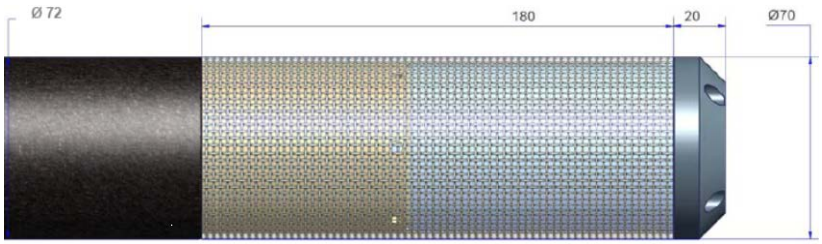

Figure 5 *Standard schematic diagram of a borehole-end interval in a 76-mm-diameter borehole*

Warning: The volume of the gas injection interval (Interval 2) given in the "design and installation of the PGZ1 experiment at Bure" (deliverable D5.4) has been more accurately assessed.

Analysis of the gas injection demonstrated inconsistencies between the theoretical volume supplied by Solexperts and what was found in the analysis.

After checking, the volumes for Interval 2 are:

- Volume of "Filter + space between pipe and filter" = 110 + 90 = 200 cm3
- Volume of "Lines" = "Volume of in-borehole lines" + "Volume of external lines" = 580 cm3,
- This gives a total equipment volume of 780 cm3.

On installation, and after initial saturation of the interval, the volume of water injected (1516 cm^3) corresponded to the total volume of the equipment and an additional volume of 1516 – 780 = 736 cm^3. This additional volume corresponded to the volume of the annular space and breakouts between the filter and the rock.

3.1.2.2 Packer seals

The hydro-mechanical packer seals have an anchoring length of 484 mm, except for the two packers next to Interval 2 of PGZ1201 which both have an anchoring length of 984 mm. The external diameter of the non-anchored packer seals is 72 mm. The resin is a natural resin and the body is made of stainless steel. The packer seals are designed for a pressure difference of 180 bar in a 76 mm borehole.

Except for the three packer seals located at the bottom of the boreholes, the packer seals are anchored in groups of two by injecting water into the (2.4 mm and 4 mm) stainless steel lines.

After packer seal anchoring, resin is injected into the inter-packer annular space. This two-component epoxy resin provides leaktightness and low system-compressibility once the resin has hardened.

For PGZ1201, only the packers around the gas-injection interval are fitted with pressure sensors (PPK01 and PPK02) which continuously record the pressure (see Figure 3).

3.2 History

The boreholes were drilled and fitted out in July 2009. In September 2009, an initial hydraulic test (HYDRO1) was performed on PGZ1201 Interval 2. The GAS1 injection phase started in February 2010 and finished in May 2011. It was comprised of six constant flowrate gas injection steps each of several (7 to 15) days duration, followed by pressure recovery phases (of 19 to 146 days). The maximum pressure reached in the last step was 91 bar. After the pressure increase phase, GAS1 was completed by a gas extraction phase (called GRE). On 5 May 2011, Interval 2 was refilled with water so that a second hydraulic test (HYDRO2) could be performed in June 2011.

Table 2 gives a simplified history of the events that occurred in the PGZ1 borehole group:

- Column 2 in the table specifies the number of days since borehole PGZ1201 was drilled.
- Columns 7 and 8 give the gas flowrates and the volumes of water injected or extracted.

Table 2 Simplified PGZ1 logbook

date	elapsed time	borehole	description	phase	duration	gas flow rate	volume of water
	days				days	mLn/min @ 273.15 K, 1 atm	cm^3
2-juil.-09	-25	PGZ1031	drilling PGZ1031				
3-juil.-09	-24	PGZ1031	equipment installation				
27-juil.-09	**0**	**PGZ1201**	**drilling PGZ1201**				
28-juil.-09	1	PGZ1201	equipment installation	saturation int 2			1516
29-juil.-09	2	PGZ1202	drilling PGZ1202				
30-juil.-09	3	PGZ1202	equipment installation				
28-août-09	32	PGZ1201	pulse test (withdrawal)	**HYDRO1 - pulse**			
14-sept.-09	49	PGZ1201	constant pressure test (injection)	**HYDRO1 - cte pressure**	5		
28-janv.-10	185	PGZ1201	water-gas exchange (N2) + cst pressure	**start GAS1**	4	variable	-810
1-févr.-10	189	PGZ1201	start gas injection 1	GRI1	11	0.5	
5-févr.-10	193	PGZ1201	increase flowrate			0.87	
12-févr.-10	200	PGZ1201	stop gas injection 1	GRIS1	19		
3-mars-10	219	PGZ1201	start gas injection 2	GRI2	15	1	
18-mars-10	234	PGZ1201	stop gas injection 2	GRIS2	20		
7-avr.-10	254	PGZ1201	start gas injection 3	GRI3	7	3	
14-avr.-10	261	PGZ1201	stop gas injection 3	GRIS3	28		
12-mai-10	289	PGZ1201	start gas injection 4	GRI4	13	1.5	
25-mai-10	302	PGZ1201	stop gas injection 4	GRIS4	29		
18-juin-10	326	PGZ1201	packer inflation				
24-juin-10	332	PGZ1201	start gas injection 5	GRI5	11	1.3	
1-juil.-10	339	PGZ1201	flow gas controller failure				
5-juil.-10	343	PGZ1201	stop gas injection 5	GRIS5	107		
20-oct.-10	450	PGZ1201	start gas injection 6	GRI6	15	1.3	
4-nov.-10	465	PGZ1201	stop gas injection 6	GRIS6	146		
30-mars-11	611	PGZ1201	start gas extraction (cte Q)	**Stop GAS1** - start GRE		-2.9	
1-avr.-11	613	PGZ1201	change gas flow rate		14	-16.9	
13-avr.-11	625	PGZ1201	gas extraction (cte P)	GRE @ cte pressure	22	variable	
5-mai-11	647	PGZ1201	stop gas extraction + compressibility test @PGZ1201PRE02	stop GRE + saturation + compressibility test			1119
27-mai-11	669	PGZ1201	compressibility test @PGZ1201PRE02	compressibility test			
6-juin-11	679	PGZ1201	packer inflation test (PPK01)				
6-juin-11	679	PGZ1201	addition PPK03				
9-juin-11	682	PGZ1201	pulse test (withdrawal)	**HYDRO2 - pulse**			
24-juin-11	697	PGZ1201	constant pressure test (injection)	**HYDRO2 - cte pressure**	6		
22-juil.-11	725	PGZ1201-1202	addition PPK04 @PGZ1201 + PPK01 to PPK04 @PGZ1202				
2-août-11	736	PGZ1201-1202	compressibility tests PGZ1202PRE01-02-03 + PGZ1201PRE01-03	compressibility tests			

3.3 Presentation of the measurements over the whole test period

3.3.1 Borehole PGZ1201

Figure 6 gives the interstitial-pressure measurements and the pressure measurements for the two monitored packers on either side of Interval 2 of PGZ1201.

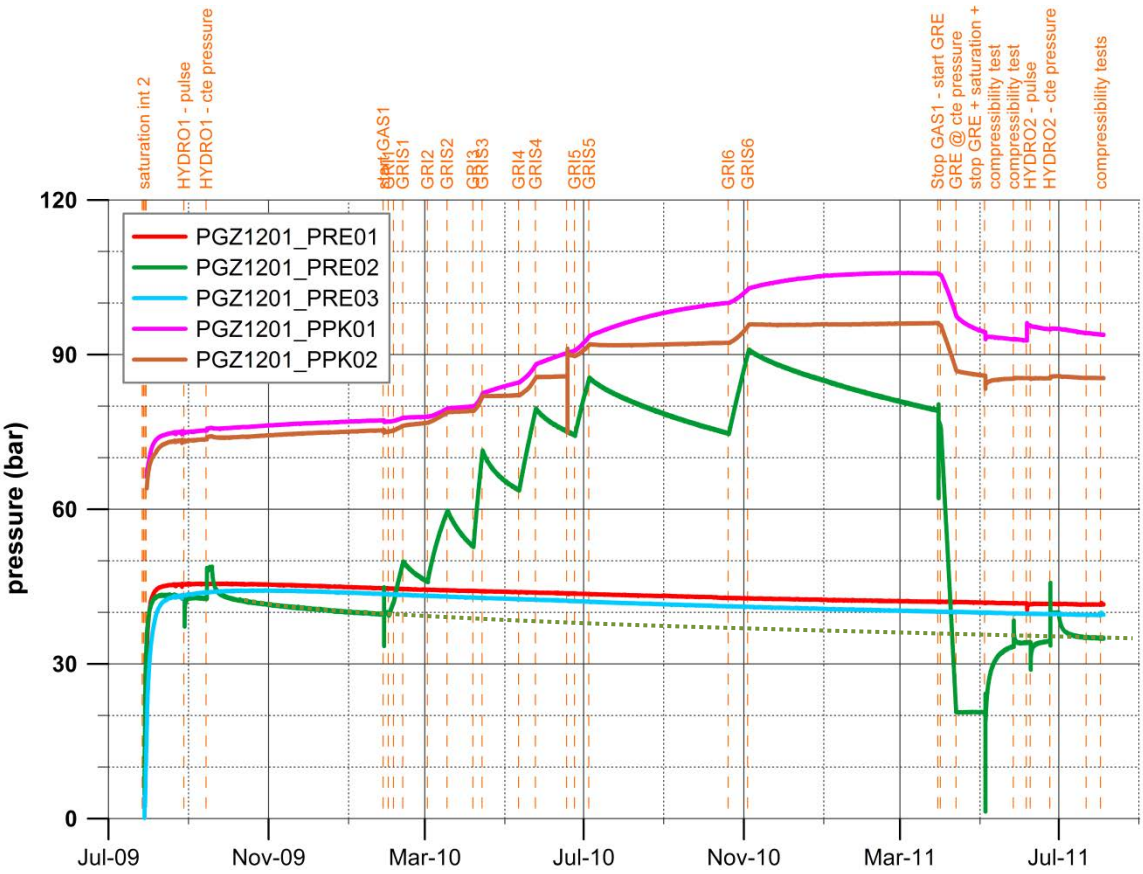

Figure 6 *Pressure measurements for the three intervals and two packers of PGZ1201 over the whole test period*

On this time chart, the following can be seen:

- A 6-month pressure monitoring period prior to the gas-injection phase,
- A 13-month period of gas injection into Interval 2,
- A one-month gas extraction phase,
- A refilling-with-water phase and (ongoing) monitoring.

The dotted vertical lines indicate the various steps listed in Table 2.

Two specific phenomena appear on this time chart.

1. The first phenomenon is the pressure reduction observed for the three intervals prior to gas injection. This reduction is continuous for Intervals 1 and 3, whereas for Interval 2, the water pressure after stabilisation reached 35 bar (beginning of August 2011), having been approximately 40 bar just prior to the gas injection phase. Table 3 gives the mean gradients from the end of December 2009 to the end of July 2011. For the measurement at Interval 2, the green dotted line represents the estimated water pressure without gas injection.

Table 3 *Pressure-reduction gradients observed in PGZ1201 for two dates*

Mean gradient in bar/day	End-of-December 2009	End-of-July 2011
PGZ1201PRE01	-0.011	-0.003
PGZ1201PRE02	-0.018	-0.002
PGZ1201PRE03	-0.009	-0.004

2. The two packers around the injection interval behave differently during the (GAS1) gas injection phase, but only from injection step 3. This will be examined in section 8.

Temperature measurements recorded in the three intervals are not given as the temperature was essentially constant, between 22.5°C and 22.6°C.

Measurements of gas flowrate are given in detail in the sections concerning the injection phase.

3.3.2 Borehole PGZ1202

Figure 7 gives the interstitial-pressure measurements for borehole PGZ1202 over the whole period.

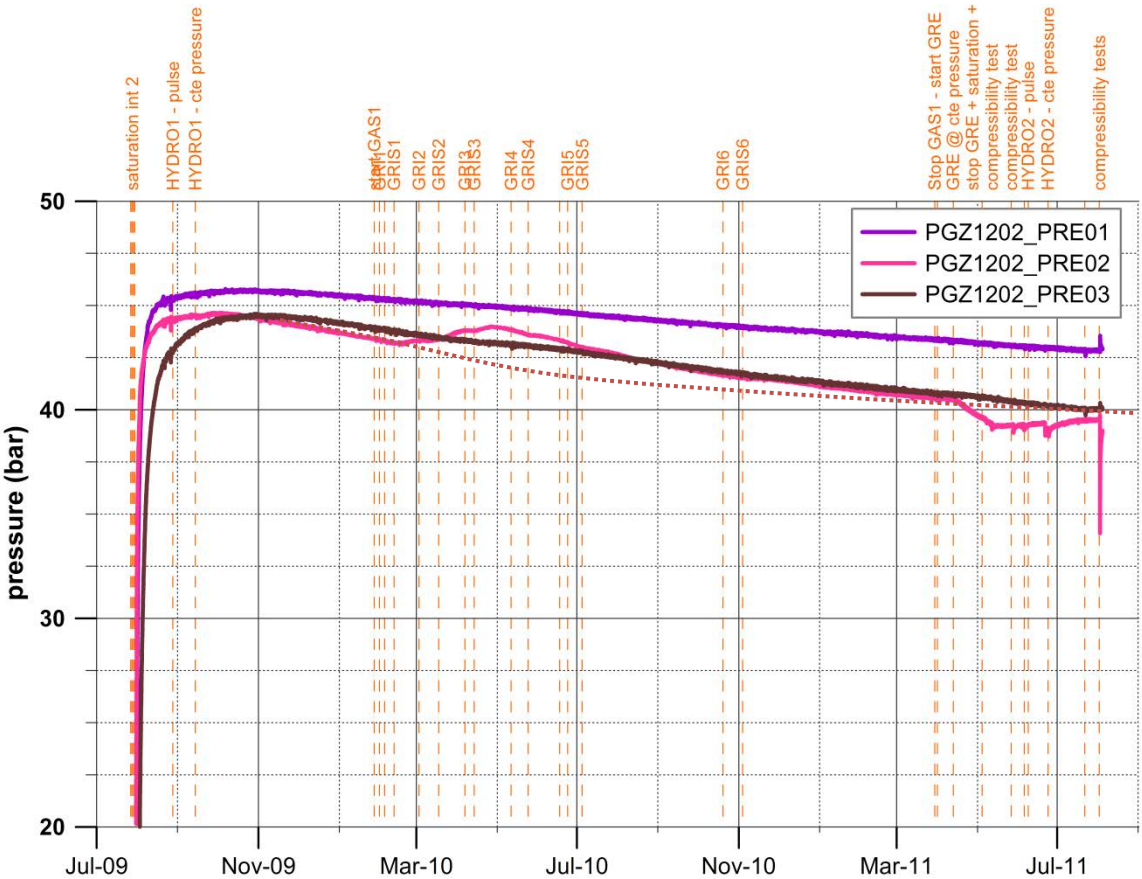

Figure 7 *Pressure measurements for the three intervals of PGZ1202 over the whole test period*

Excluding the hydraulic interference associated with gas injection in the neighbouring borehole, the same pressure-reduction phenomenon appears over all three intervals. Table 4 gives the gradients observed for two dates (end-of-December 2009 and July 2011). The dotted curve gives the estimated water pressure without gas injection for PGZ1202PRE02. This reduction in pressure is also damped over time.

Table 4 Pressure-reduction gradients observed in PGZ1202 for two dates

Mean gradient in bar/day	End-of-December 2009	End-of-July 2011
PGZ1202PRE01	-0.005	-0.004
PGZ1202PRE02	-0.011	-0.002
PGZ1202PRE03	-0.009	-0.006

This phenomenon is due to the cone of depression around borehole PGZ1031 (drainage phenomenon). This point is elaborated in Section 4.2.2.

3.3.3 Borehole PGZ1031

Borehole PGZ1031 measures displacements along the borehole axis using 20 magnetic rings, which are cast in the cemented annular space and distributed along the borehole. Figure 8 shows the distribution along the borehole and the numbering of the anchors, along with their initial positions in French "Lambert 2" coordinates. Note that Figure 3 shows the position of the anchors with respect to the other two boreholes.

The distribution of the anchors has been chosen to measure the opening of the crack that will be created during the GAS2 Phase – under the highly-probable assumption that the crack's propagation plane passes through this borehole. This is why the magnetic rings have been densely distributed around Interval 2 of PGZ1201, both vertically and horizontally from this interval.

position initiale des points de mesure				
distance en longueur forée	X	Y	Z	dénomination SAGD
m	m	m	m	
0.000	823221.043	1091617.887	-125.415	tête forage
8.360	823226.052	1091620.426	-131.590	**PGZ1031_DFO_20**
13.360	823229.048	1091621.942	-135.295	**PGZ1031_DFO_19**
14.110	823229.496	1091622.170	-135.852	**PGZ1031_DFO_18**
14.860	823229.945	1091622.398	-136.408	**PGZ1031_DFO_17**
15.610	823230.394	1091622.625	-136.964	**PGZ1031_DFO_16**
16.360	823230.843	1091622.853	-137.520	**PGZ1031_DFO_15**
16.860	823231.141	1091623.005	-137.891	**PGZ1031_DFO_14**
17.360	823231.440	1091623.157	-138.262	**PGZ1031_DFO_13**
17.660	823231.620	1091623.249	-138.484	**PGZ1031_DFO_12**
17.960	823231.800	1091623.340	-138.706	**PGZ1031_DFO_11**
18.260	823231.979	1091623.431	-138.929	**PGZ1031_DFO_10**
18.560	823232.158	1091623.521	-139.152	**PGZ1031_DFO_09**
18.860	823232.337	1091623.612	-139.375	**PGZ1031_DFO_08**
19.360	823232.635	1091623.764	-139.746	**PGZ1031_DFO_07**
19.860	823232.934	1091623.916	-140.118	**PGZ1031_DFO_06**
20.360	823233.232	1091624.068	-140.489	**PGZ1031_DFO_05**
20.860	823233.531	1091624.220	-140.860	**PGZ1031_DFO_04**
21.360	823233.830	1091624.373	-141.230	**PGZ1031_DFO_03**
22.110	823234.278	1091624.601	-141.787	**PGZ1031_DFO_02**
22.860	823234.727	1091624.829	-142.343	**PGZ1031_DFO_01**

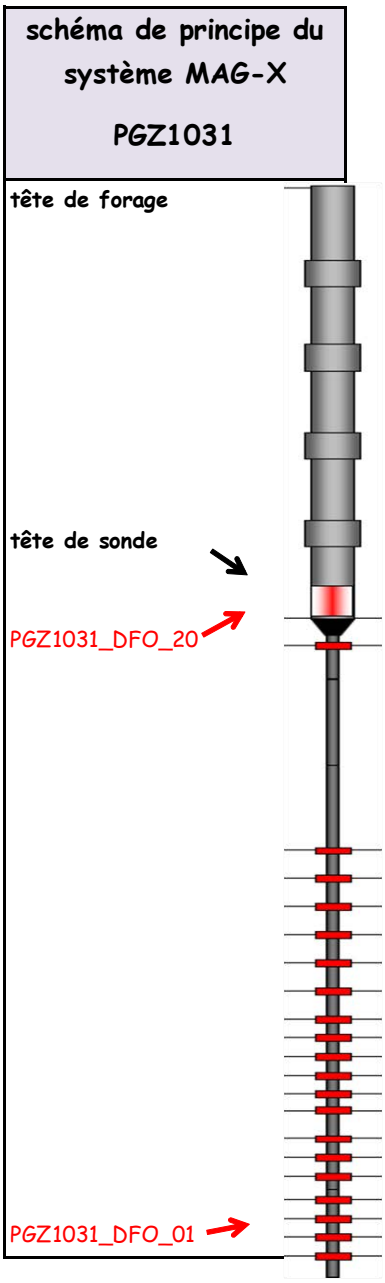

Figure 8 Anchor positions for borehole PGZ1031

Figure 9 shows the relative displacements measured over the whole test period. These relative displacements are given with respect to anchor “01" at the bottom of the borehole, which is assumed fixed.

The displacements measured since the measurement system was installed are negative, i.e. they represent a displacement of the measurement points towards the drill head and thus towards the side wall of the “experimental drift (GEX)”. The displacements are very small, less than 0.6 mm for the anchor located approximately 8 m from the GEX drift wall. Various peaks appear in the measurements, which may be associated with shocks at the drill head or thermal expansions of the system.

These peaks attenuate with depth, due to the calculation method based on a fixed point at the bottom of the borehole.

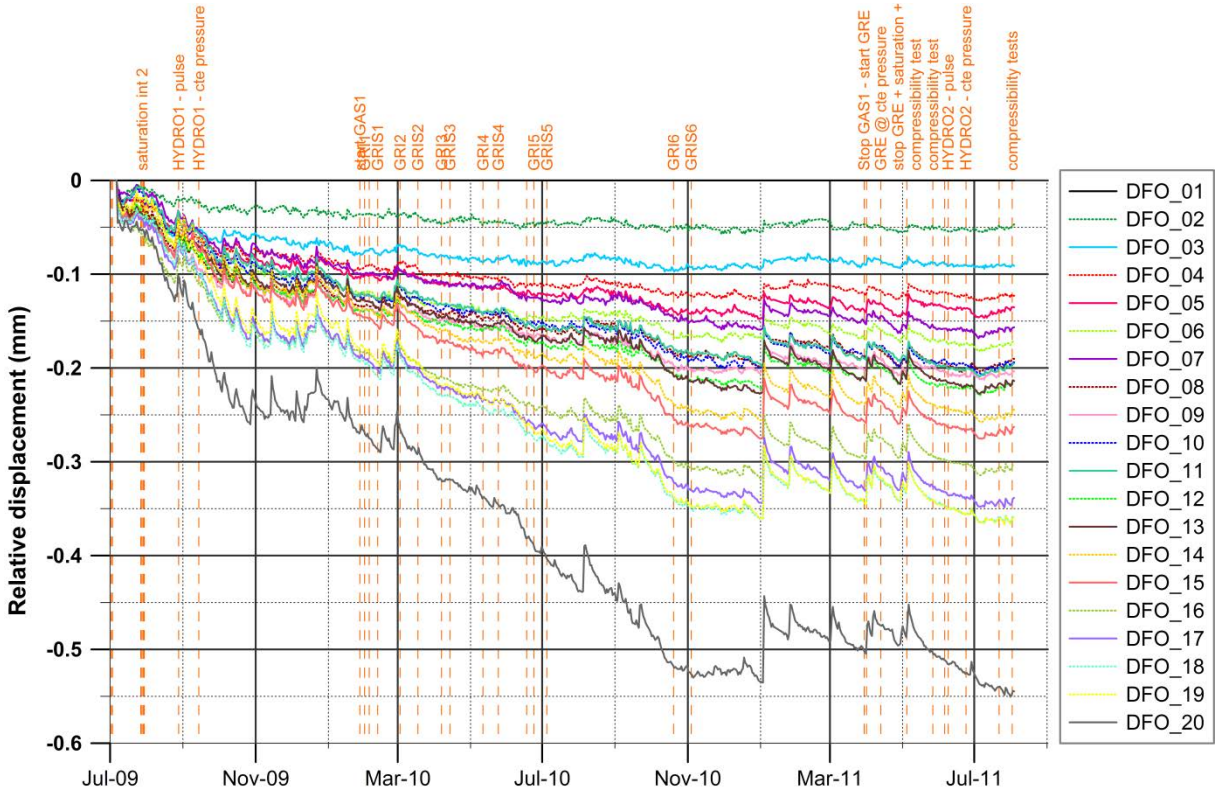

Figure 9 *Monitoring of relative displacement measurements for PGZ1031 (t_0 = installation) over the whole period*

There were rapid displacements in the first few days after installation of the measurement system; these could be associated with the setting of the cement (shrinkage) or mechanical rearrangement of grains around the borehole.

By defining t_0 as 1 August 2009, the problem of this initial phenomenon, which is not a real displacement of the argillite, is avoided. The monitoring of relative displacements is shown in Figure 10.

The numerous peaks observed on Figure 10 are seen to be attenuated but the amplitudes of the displacements are a bit larger for anchors 19 and 20. The displacement amplitudes are inversely proportional to the distance between the drift's side wall and the anchor, which agrees with observations made elsewhere with standard extensometers which show greater convergence near to the side wall.

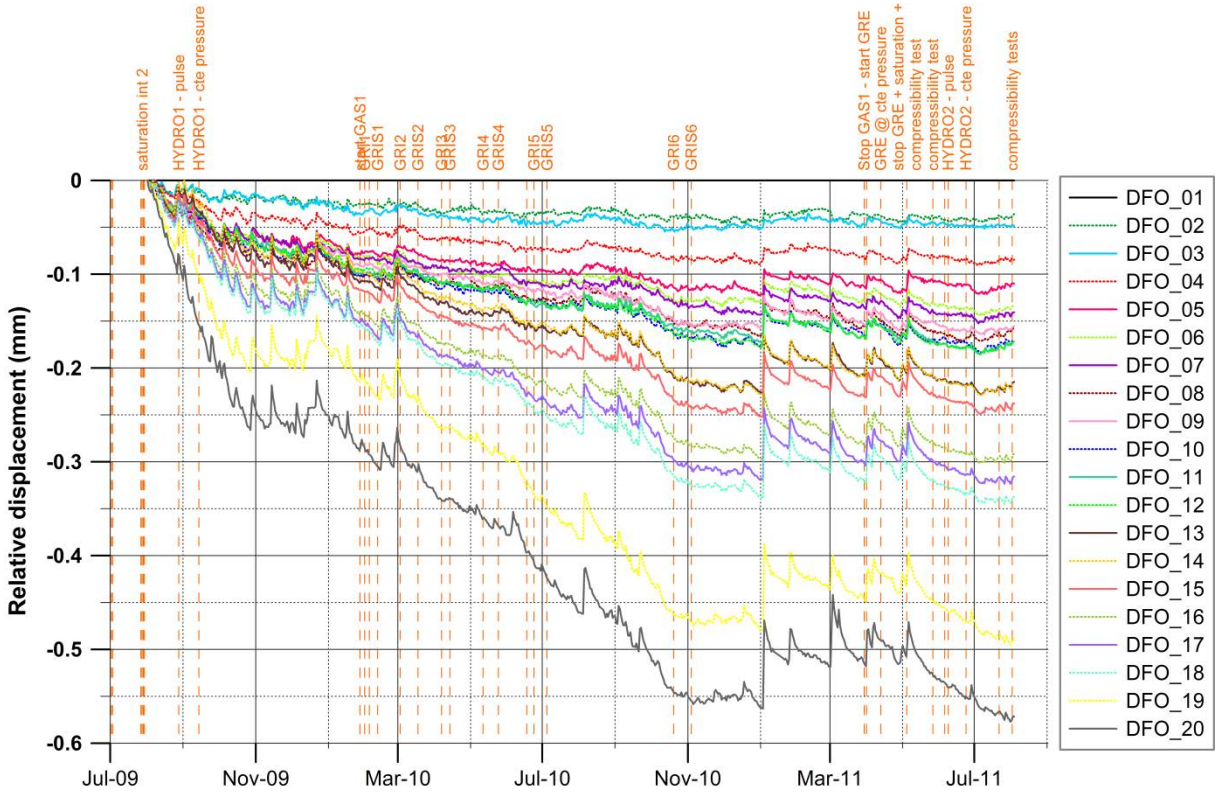

Figure 10 *Monitoring of relative displacement measurements for PGZ1031 (t_0 = 1 August 2009) over the whole test period*

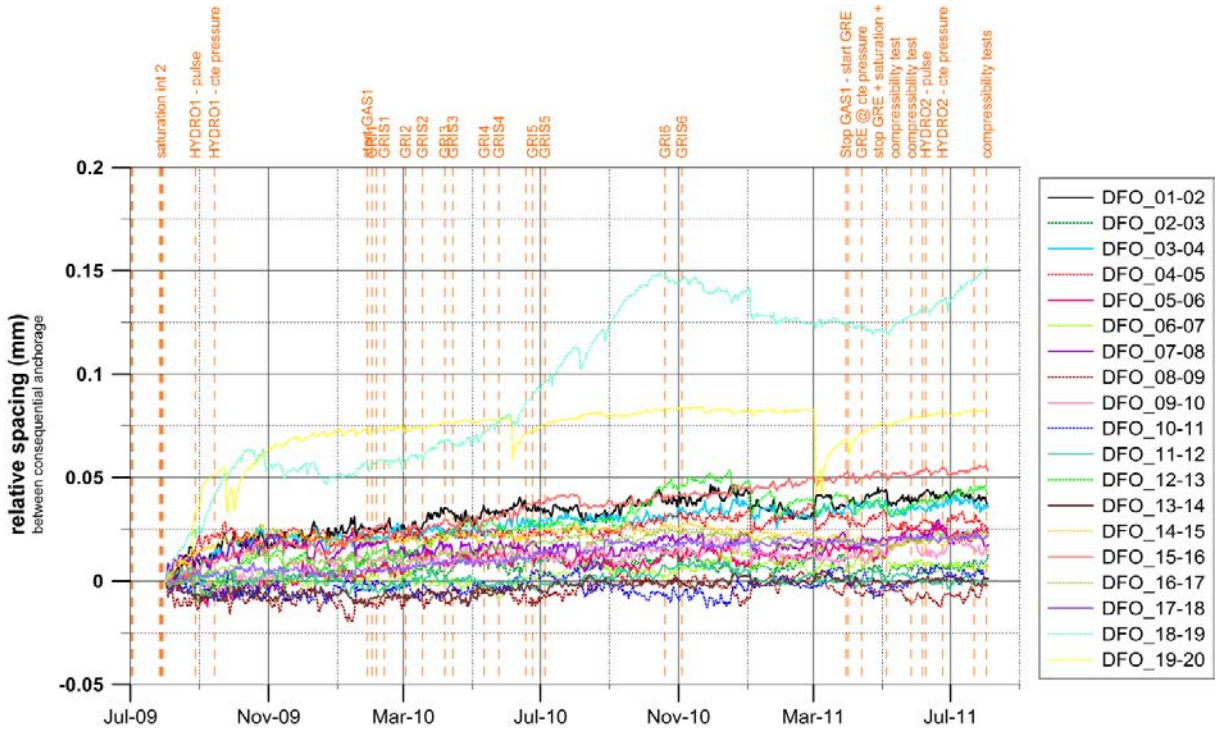

Figure 11 *Relative discrepancies between two consecutive anchorages (t_0 = 1 August 2009) over the whole test period; positive discrepancy = elongation*

From Figure 10 we can calculate the relative spacing between two consecutive anchors (Figure 11) with respect to their initial spacing (t_0 = 1 August 2009).

Only the two anchors which are closest to the GEX drift show a change in separation significantly different from that of the other anchors. The distance between anchors 18 and 19 is atypical with no obvious explanation.

For anchors 01 to 18, the distances change slowly with a slight linear increase in their spacing. The maximum gradient is 50 µm/day (anchors 15 and 16). As their initial spacing was 0.3 m, this gives a maximum strain rate of 1.9×10^{-12} s^{-1}.

This value of initial strain rate, which is associated with the convergence of the rock mass toward the GEX drift, is consistent with the estimates given by models for this distance from the side wall for nearly 5 years following the excavation of the drift.

In the area around Interval 2 of PGZ1201, the measurements of displacement do not demonstrate any particular phenomena in the argillite which could be associated with gas injection, i.e. any strains which may be caused by the gas injection tests at a distance of 1.14 m from the chamber are much smaller than the strains associated with convergence towards the GEX drift. For this reason, these measurements will not be analysed in greater detail in this document.

4. Period prior to the gas injection phase

4.1 Hydraulic tests in Interval 2 of PGZ1201

A series of hydraulic tests (HYDRO1), comprising a pulse-withdrawal test and a constant overpressure test were performed in August/September 2009 in Interval 2 of PGZ1201. The dark green curve in Figure 13 shows the pressure measurements in this interval. Computer analysis was applied to these two tests, to adjust the simulations to the measurements.

The flow model adopted around the test interval is a composite radial flow model with an inner zone of higher permeability than the outer zone. This inner zone represents the excavated damaged zone (EDZ) and is 4cm thick[1]. The parameters obtained for the formation are summarised in the table below:

Table 5 Parameters for the rock around Interval 2 of PGZ1201 (HYDRO1)

K_{inner} [m/s]	K_{outer} [m/s]	Pi [bar]	r_d [m]	$S_{s\ inner}$ [m^{-1}]	$S_{s\ outer}$ [m^{-1}]	Ctz [Pa^{-1}]
6.4×10^{-11}	$K_{ref} = 2.6 \times 10^{-13}$ **8.0×10^{-14} – 6.0×10^{-13}**	45.6	0.04	1.0×10^{-6}	3.0×10^{-6}	2.0×10^{-9}

The difference between the specific storage (S_s) values in the inner and outer zones is not significant.

The permeability of the outer zone is representative of undamaged argillite. The radius of influence of the series of pulse tests and the constant pressure test is approximately 1.5 m.

[1] In the event of using a radial composite model, the inner zone is limited to a maximum extension of 10 cm from the borehole wall (rd < 0.1m + borehole radius). In the presence of a formation assumed to be fully saturated and undisturbed, the specific storage is limited to a range of 1×10^{-6} m^{-1} to 3×10^{-6} m^{-1} (reference values for undamaged Callovo-Oxfordian). In the event of the assumption of desaturation or damage to the formation at the intervals, the specific storage may vary up to level of porosity (i.e. approximately 15% for argillite). The methodology and assumptions follow those given in Report D.RP.0CPE.09.009 "*Expérimentation OHZ / Optimisation des contraintes pour l'analyse des tests hydrogéologiques*" (OHZ experiment / Optimisation of constraints for the analysis of hydro-geology tests).

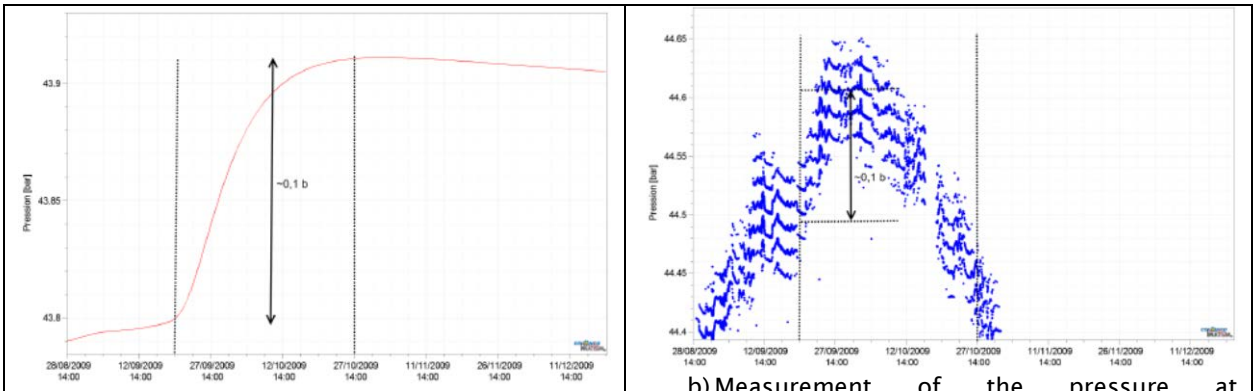

a) Simulation of hydraulic interference with the parameters from Table 5 and linear detrending

b) Measurement of the pressure at PGZ1202PRE02 and demonstration of hydraulic interference

Figure 12 Observed and simulated hydraulic interference for the constant pressure test

The tests seemed to produce very slight interference, of the order of 0.1 bar, between Interval 2 of borehole PGZ1201 and Interval 2 of borehole PGZ1202. It was possible to reproduce this interference by simulating the tests, but a linear correction of the pressure transient was required (Figure 12).

4.2 Interstitial-pressure measurements (PGZ1201 & PGZ1202)

4.2.1 Measurements

Figure 13 shows the interstitial-pressure measurements for the 6 intervals in boreholes PGZ1201 and PGZ1202 up to the beginning of gas injection.

In Interval 2 of PGZ1201, the maximum pressure reached was 43.3 bar. The maximum pressure measured in the five other measurement chambers was between 44.2 bar and 45.8 bar. Following this maximum, a more or less gradual reduction in interstitial pressure was observed for all the measurement intervals (see also Figure 6 and Figure 7 and, for the gradients, Table 3 and Table 4).

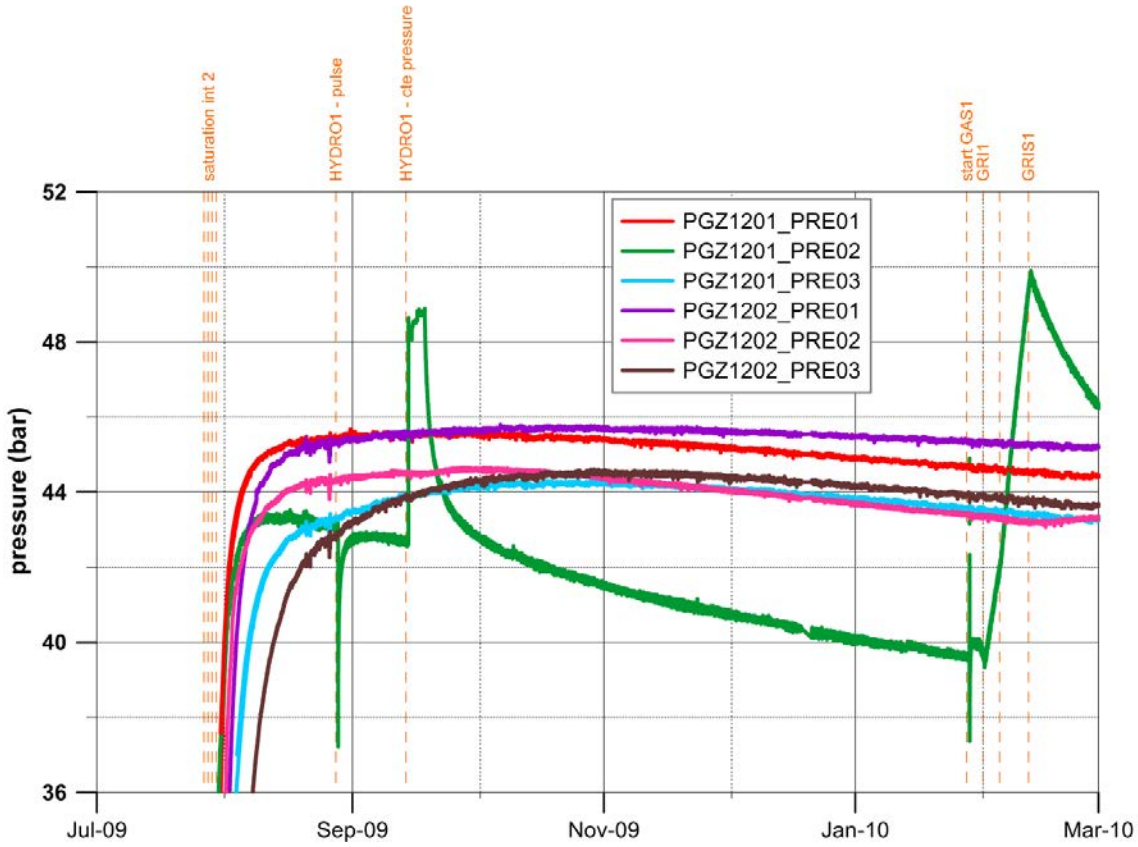

Figure 13 *Measurements of PGZ1201 and PGZ1202 interstitial pressure between July 2009 and February 2010*

4.2.2 Drainage phenomena

In terms of amplitude and kinetics, the "Interval 2"s of PGZ1201 and PGZ1202 were the most affected while their respective "Interval 1"s were the least affected. At end-of-December 2009, the pressure-reduction gradient was approximately -0.018 bar/day for PGZ1201PRE02 and -0.005 bar/day for PGZ1202PRE01. On the other hand, in July 2011 (see Table 3 and Table 4), the gradients of the intervals closest to PGZ1031 (PGZ120XPRE02) are the smallest.

From Table 1, which gives the distances between the measurement chambers and borehole PGZ1031, the two "Interval 2"s are the closest while the two "Interval 1"s are the furthest from PGZ1031. This strong correlation between the distance to borehole PGZ1031 and the kinetics and amplitude of pressure reduction leads to interpreting this reduction in interstitial pressure as an effect of drainage via the cemented annular space of PGZ1031.

"design and installation of the PGZ1 experiment at Bure" (deliverable D5.4) had already suggested this hypothesis and a computer analysis using an axisymmetrical model was performed by AF CONSULT - INTERA to assess its likelihood (D.RP.0CPE.11.0001). This computer analysis was performed in two stages (i) an initial simplified analysis for saturated flow with a constant pressure boundary equal to 1 bar at the draining borehole, followed by (ii) a two-phase flow analysis with a sensitivity analysis taking into account saturation conditions in the cement of the draining borehole down as far as the drift.

i. The saturated flow analysis demonstrated that a constant pressure boundary at the PGZ1031 borehole allows the gradients observed in December 2009 to be reproduced (Figure 14). The parameters used for this simulation were the same as the parameters obtained to calibrate the measurements to the HYDRO1 tests (see Table 5).
ii. The two-phase flow analysis demonstrated high sensitivity to the permeability of the cement and low sensitivity to the damaged zone of borehole PGZ1031.

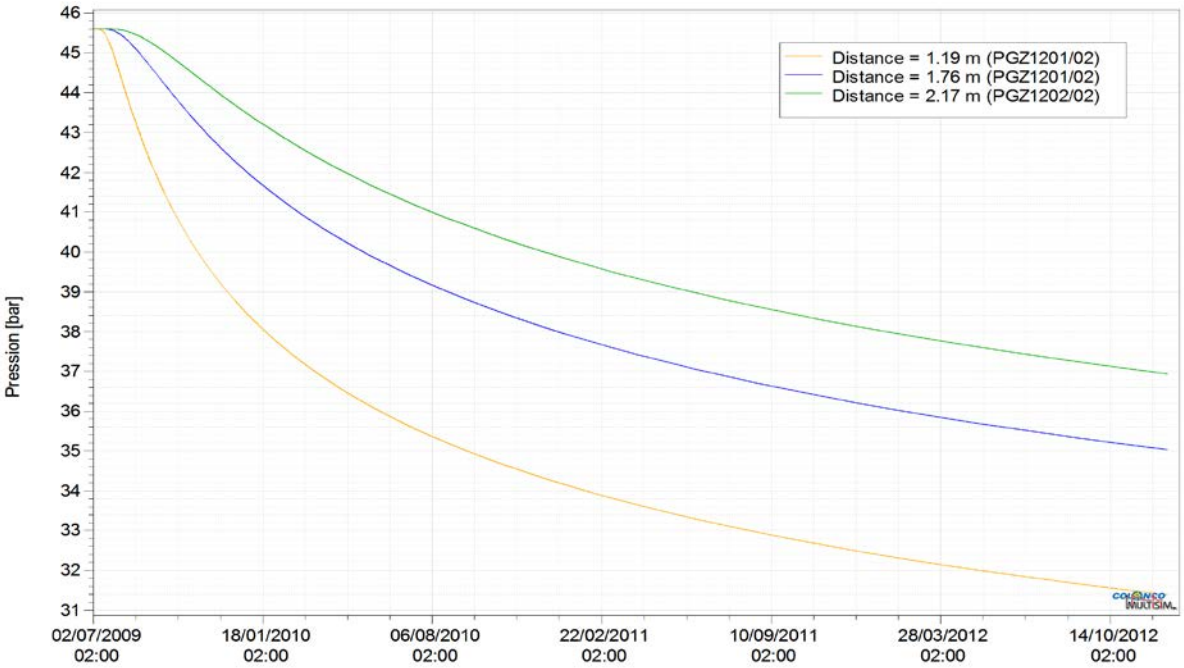

Figure 14 *Simulation of the changes in pressure at various distances from PGZ1031 for a drainage taken as equivalent to a constant pressure boundary equal to atmospheric pressure*Figure 14 shows damping of the drainage phenomenon over time. Strictly speaking, it should not have been necessary to apply a linear correction during analysis of the HYDRO1 hydraulic tests. However, over the duration of the two hydraulic tests (approximately 3 weeks) this linear correction remains acceptable.

Thus, it is possible to simulate the drainage effect of borehole PGZ1031 using the parameters taken from the HYDRO1 test phase. This drainage effect can be seen as an additional interference test, which confirms the hydraulic characteristics around the boreholes at a metre-scale.

4.3 Pressure measurements for the (PGZ1201) packers

4.3.1 Measurements

Figure 15 shows the pressure measurements for the packers around Interval 2 of PGZ1201, and the pressure measured in Interval 2 for six months prior to gas injection. Measurement PPK01 corresponds to the pressure measurement for the packer located at the lower end of Interval 2 while measurement PPK02 corresponds to the one located at the upper end.

The behaviour of the two packers is very similar. After a brief rising-pressure phase at the packers, corresponding to the rapid rise in pressure in the interval, the pressure continues to slowly increase at the packers while the interstitial pressure in the interval slowly decreases. This lack of correlation between the interstitial pressure and the pressure at the packers indicates a decrease in packer volume, due to convergence of the borehole wall.

During this slow rising-pressure phase at the packers, pressure simulations during (HYDRO1) hydraulic tests induced a pressure response in the packers (squeeze effect).

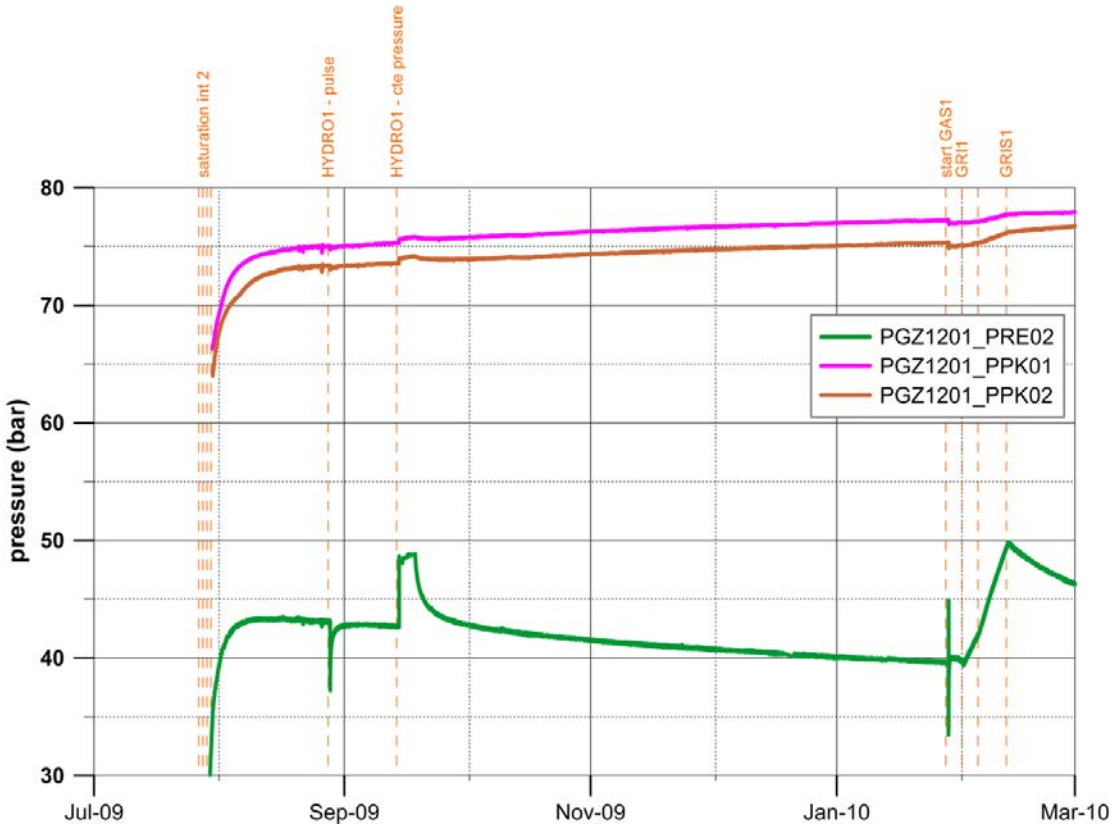

Figure 15 *Pressure measurements for the packers surrounding Interval 2 of PGZ1201 and pressure measurement at Interval 2 between July 2009 and February 2010*

4.4 Convergence phenomena

4.4.1 At the packers

The pressure variations measured over 6 months, between 24 August 2009 and 18 January 2010, mean that the volume and diameter variation of each packer can be calculated by assuming that the packers are cylindrical[2], with an initial volume of 457.52 cm^3, and that its isothermal compressibility in water is 4.9×10^{-5} bar^{-1}.

Table 6 *Variations in the volume and diameter of packers PPK01 and PPK02 between 24 August and 18 January*

	Packer pressure (bar)		Pressure variation (bar)		Volume variation (mm^3)		Diameter variation (µm)	
	PPK01	PPK02	PPK01	PPK02	PPK01	PPK02	PPK01	PPK02
24/08/2009	74.97	73.3	-	-	-	-	-	-
18/01/2010	77.2	75.27	2.23	1.97	-50	-44	-0.43	-0.38

[2] Internal diameter 72 mm, external diameter 76 mm, and packer length 984 mm.

The calculated diameter variation is an underestimate as the packer pressure is also affected by the interstitial pressure which is reducing. Thus, at constant interstitial pressure, packer pressure should increase more. Ultimately, the actual convergence of the borehole at the packers remains very small (micron-scale).

4.4.1.1 At the filter

The amplitude of the convergence at the interval filter is difficult to estimate because the convergence is not limited by the compressibility of the packers. Using the measurements performed on unsleeved HLW cells where the maximum convergence 6 months after excavation was approximately 2% to 3% of initial diameter, the maximum estimated convergence would be approximately 1.5 mm at the diameter (for an initial diameter of 76 mm), assuming all things equal otherwise. As the diameter of the filter is 70 mm, a cylindrical annular space 2.25 mm wide remains before the Interval 2 gas injection phase begins, i.e. a volume of 511 cm^3.

This point is discussed in more detail in Section 7.2.

5. Gas-water exchange phase

The "GAS1" phase began on the 28 January 2010 with the gas-water exchange phase in Interval 2 of PGZ1201.

5.1 Measurements

Interval 2 of PGZ1201 was filled with gas on 28 January 2010. To fill the interval with gas without excessively disturbing the interval's near-field pressure, water was flushed from the interval by a series of gas injections.

As seen on Figure 16, as the measured interstitial pressure in the interval (green curve) was 39.6 bar, several gas pressure steps were used (red curve = gas pressure) to remove the maximum amount of water. The interstitial pressure in the interval was measured via a hydraulic line connected to the control panel where the sensor was located. The gas pressure measurement was performed in the gas module itself (see Appendix 1).

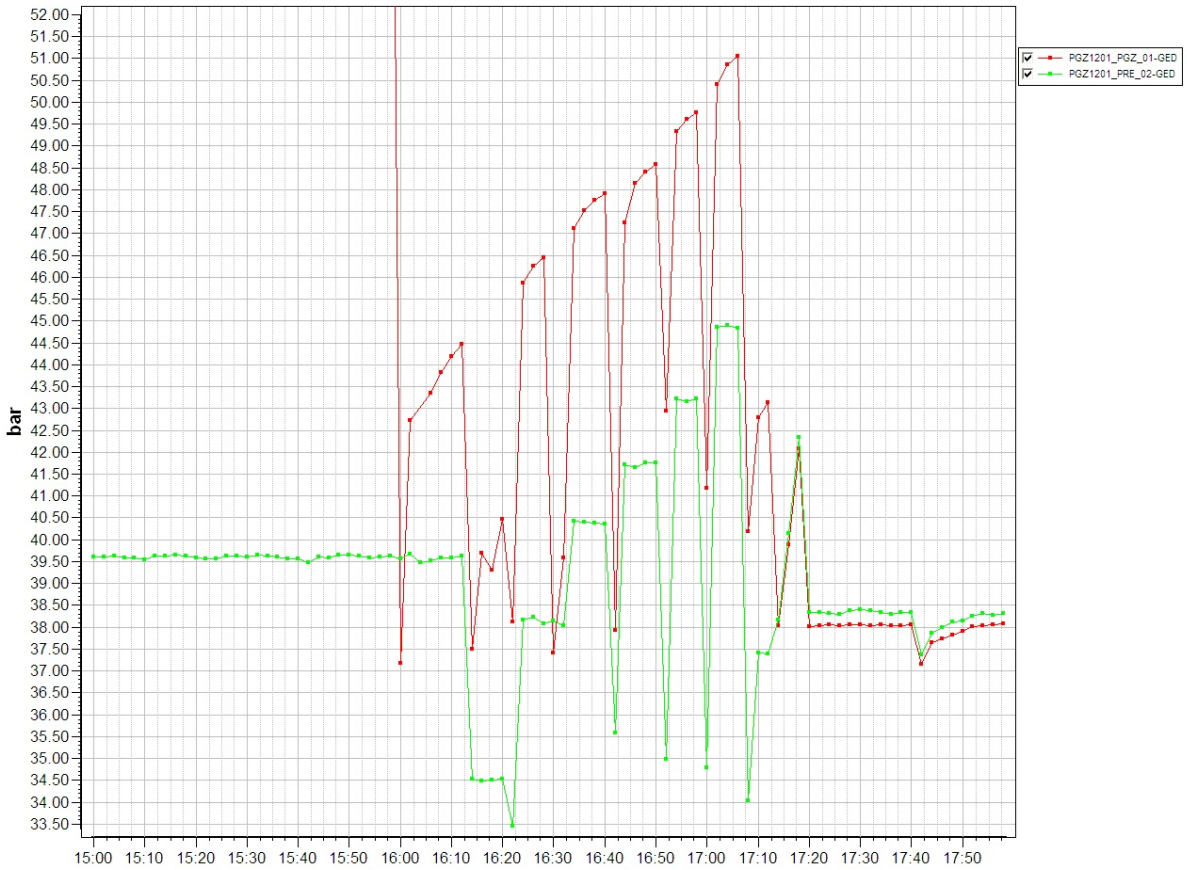

Figure 16 *Measurements of water and gas pressure during the water-gas exchange phase for Interval 2 of PGZ1201 (28 January 2010)*

During this phase, which lasted about an hour, the quantity of gas injected was not measured (pressure and not injection flowrate was monitored) but the final quantity of water extracted could be measured; this was 810 cm^3.

Next, gas injection continued by injecting a pressure-controlled flowrate via a gas flowrate regulator (pressure setpoint: 40 bar)[3]. This constant-pressure injection lasted until 1 February 2010. The quantity of gas injected was 0.09 moles of nitrogen.

The gas pressure in the interval was raised to 40 bar, i.e. a pressure greater than the water pressure before water-gas exchange. Next, despite the pressure setpoint, the pressure reduced by 0.5 bar between the 31 January 2010 and the 1 February 2010 without the regulator being able to compensate for this reduction. This small pressure drop cannot be explained by a thermal effect because the temperature in the GED drift had increased (by about 4°C) during the weekend of the 30 and 31 January 2010 as the drift ventilation system had shut down.

[3] Appendix 1 and Appendix 2 describe the type of gas flowmeter used and its operating principles.

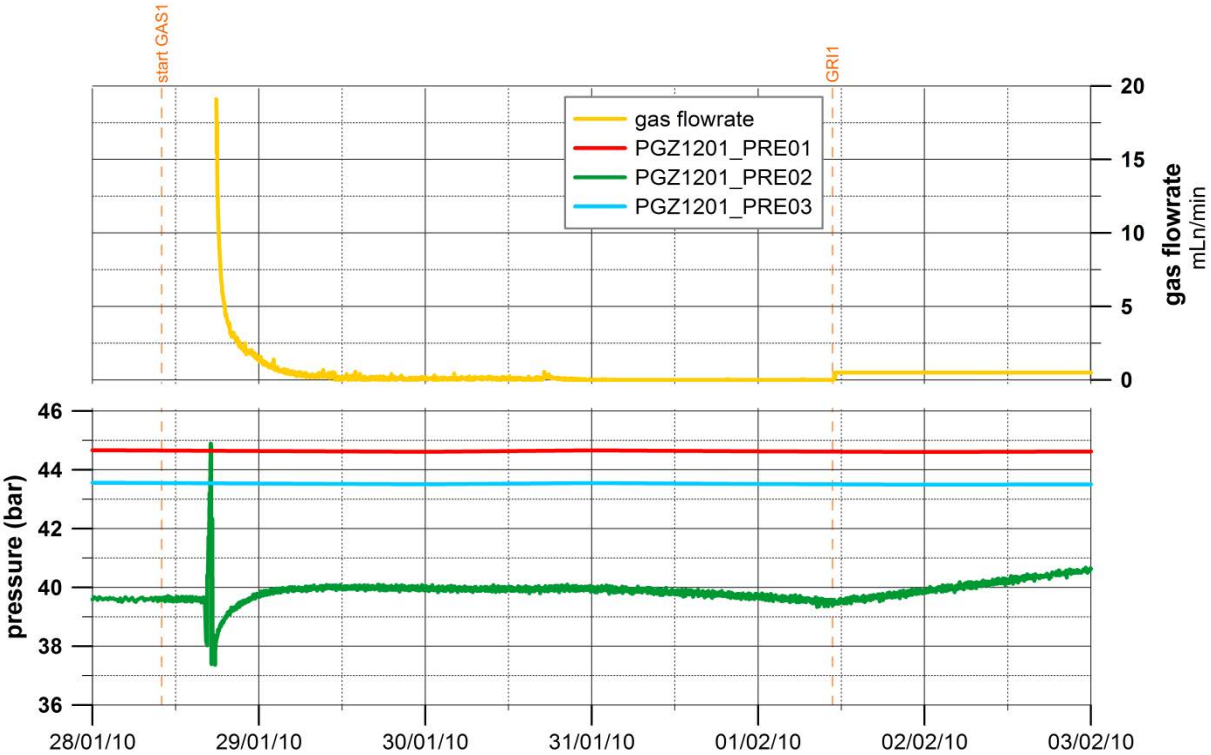

Figure 17 *Monitoring gas pressure and flowrate from 28 January 2010 to 1 February 2010*

A possible explanation for this reduction in pressure is given in Section 6.2.1.2.

5.2 Volume of Interval 2

Knowledge of the volume occupied by the gas in Interval 2 of PGZ1201 when the GAS1 injection phase began is essential for analysing this phase. A volume of residual water may remain in the interval and this could be moved when the gas pressure is increased.

During the gas injection phase, the interval can be broken down into various volumes (Figure 18), namely:

- Volume V_1: volume of the hydraulic lines from the control panel (located in the GED drift) to the interval. V_1 is equal to 580 cm³ after corrections are applied (see Section 3.1.2.1).
- Volume V_2: volume of the test interval, which is equal to the volume of the filter porosity (110 cm³) plus that of the annular space between the inner pipe and the filter (90 cm³), i.e. 200 cm³.
- Volume V_3: volume of the space between the filter and the borehole wall, which is equal to the volume of the annular space plus the volume of any breakouts. This volume can be calculated by subtracting the combined volumes V_1 and V_2 from the quantity of water used when filling Interval 2 with water on the 28 July 2009, i.e. 1516 – 780 = 736 cm³. However, this volume (V_3) could change over time due to the convergence of the borehole wall. Thus, the value of 736 cm³ for volume V_3 is a maximum value.
- Volume V_4: volume in the gas injection module between the small flowmeter (DGZ01) and the control panel; V_4 is 24 cm³.

The total maximum volume of Interval 2 of PGZ1201 is equal to the sum of these four volumes, i.e. volume $V_{int2\,max}$ = 1540 cm³.

Volume of the gas module between the small flowmeter and the control panel
V_{mg} = 24 cm³

V_1: volume of the hydraulic lines from the control panel to the test interval
V_1 = 580 cm³

V_2: volume of test interval (filter 110 cm³ + inner pipe 90 cm³)
V_2 = 200 cm³

V_3: volume between the filter and the borehole wall (annular space + breakouts).
This volume can vary over time.
$V_{3\,max}$ = 780 cm³

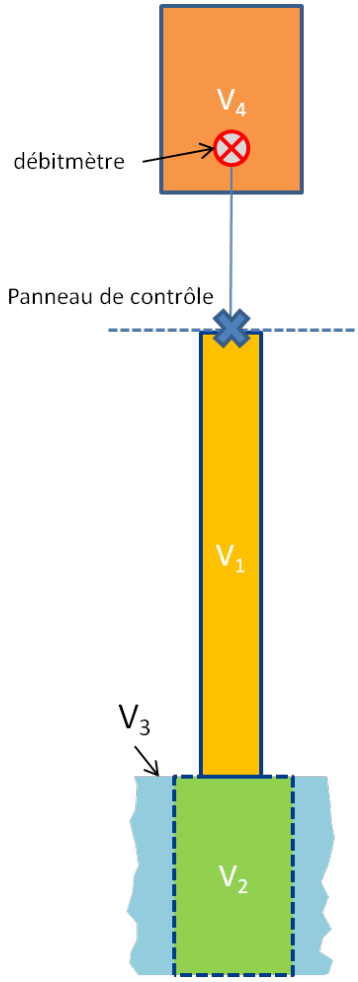

Figure 18 *Schematic drawing of the various volumes that make up Interval 2 of PGZ1201*Conversely, the technology volume (V_1 + V_2 + V_4 = 804 cm³) is the minimum total volume of Interval 2 of PGZ1201, assuming total convergence around the filter.

Now, the volume of water extracted by gas flushing was 810 cm³. As the borehole slopes downwards from the drift (-35.4°), it was not possible to extract all the water contained in this interval. Residual water remained in the lower part. This also means that convergence had not yet totally filled the annular space around the filter.

5.3 Pressure variation

The gas flowrate data and the ideal gas law can be used to calculate the pressure variation created over time in a constant volume. The volume of Interval 2 available for the gas phase is between the upper and lower limits specified above: 804 cm³ and 1540 cm³. Thermal equilibrium between the various volumes (V_1 to V_4) is assumed, with a uniform temperature of 22.5°C that is stable over time.

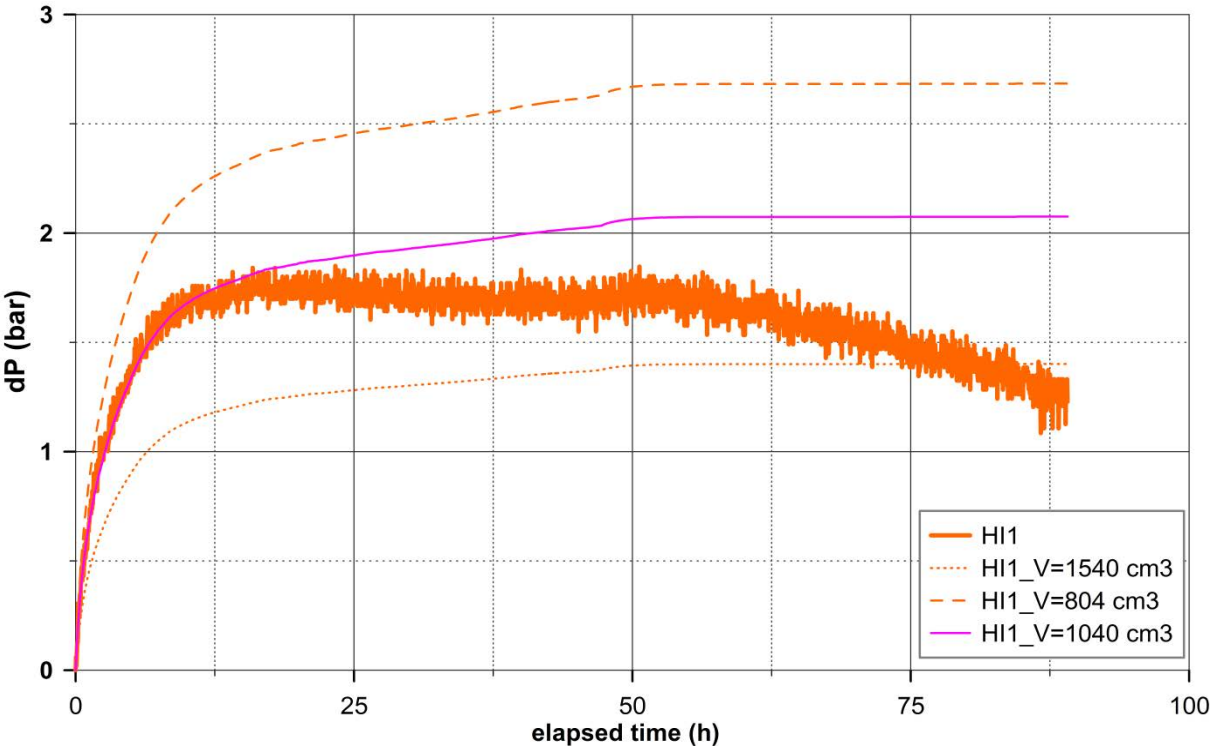

Figure 19 *Pressure variations as measured and as calculated for constant volume for injection at constant pressure*

Figure 19 shows that the pressure differences calculated for the two extreme volumes nicely contain the measured pressure variation, except towards the end (beyond 75 hours). It is possible to deduce the gas volume of Interval 2 that gives the best fit (pink curve). This best fit is obtained for a gas volume of 1040 cm^3. However, this best fit diverges beyond 12 hours after the start of injection at constant pressure.

This gas volume (1040 cm^3) is significantly larger than the volume of water extracted (810 cm^3). This shows that the various gas flushing operations (see Figure 16) pushed the water into the rock and produced 230 cm^3 of volume available for gas in the interval.

After 12 hours of gas injection with a monitored flowrate, the pink curve (best fit) deviates from the orange curve (measurement). This effect demonstrates an increase in the volume available for the gas at the expense of the volume of residual water. In Section 6.2.1.2, it will be seen that the variation of overall volume during this period is 1150 – 1040 = 110 cm^3.

This volume of 1150 cm^3 is significantly lower than the theoretical maximum volume of the interval (1540 cm^3). This means that, during this phase, the volume occupied by the gas does not exceed the maximum theoretical volume of the interval and that there is no gas penetration into the rock.

From this method, it is accepted that the gas volume in the interval is clearly between the two extremes given above and that its volume is 1040 cm^3. This method will be used for analysis of the injection steps to detect, in the pressure variations measured, the part associated with the compressibility of the gas in a constant volume and that associated with a real change in the volume of the system.

6. Rising gas pressure phases

Six constant-flowrate gas injection steps were performed during the GAS1 phase. Each injection step was followed by a pressure recovery phase.

In the rest of the document, the injection steps will be labelled "GRI", for example GRI3 means injection step 3. Pressure recovery phases will be labelled "GRIS".

The duration, amplitudes and quantities of gas injected for the GRIx and GRISx steps are summarised in Table 7:

Table 7 Summary of the GRIx and GRISx rising pressure steps

Step	Start date for step	Step duration	Initial pressure	Final pressure	dP	Mean flowrate	Quantity of nitrogen injected
		Days	Bar	Bar	Bar	ml_n/min	mol
GRI1	01/02/2010	11	39.5	49.9	10.4	0.5 then 0.9	0.53
GRIS1	12/02/2010	19	49.9	45.9	-4.0		
GRI2	03/03/2010	15	45.9	59.8	13.9	1.01	0.98
GRIS2	18/03/2010	20	59.8	52.7	-7.1		
GRI3	07/04/2010	7	52.7	71.4	18.7	2.97	1.34
GRIS3	14/04/2010	28	71.4	63.6	-7.8		
GRI4	12/05/2010	13	63.6	79.6	16.0	1.5	1.24
GRIS4	25/05/2010	30	79.6	74.4	-5.2		
GRI5	24/06/2010	11	74.4	85.6	11.2	1.3	0.88
GRIS5	05/07/2010	107	85.6	74.7	-10.9		
GRI6	20/10/2010	15	74.7	91.0	16.3	1.3	1.28
GRIS6	04/11/2010	146	91.0	79.2	-11.8		

6.1 Measurements

6.1.1 Interstitial pressures, gas pressure and flowrate

Figure 20 shows the pressure measurements at the three measurement intervals in PGZ1201 and the measured gas flowrate between January 2010 and May 2011.

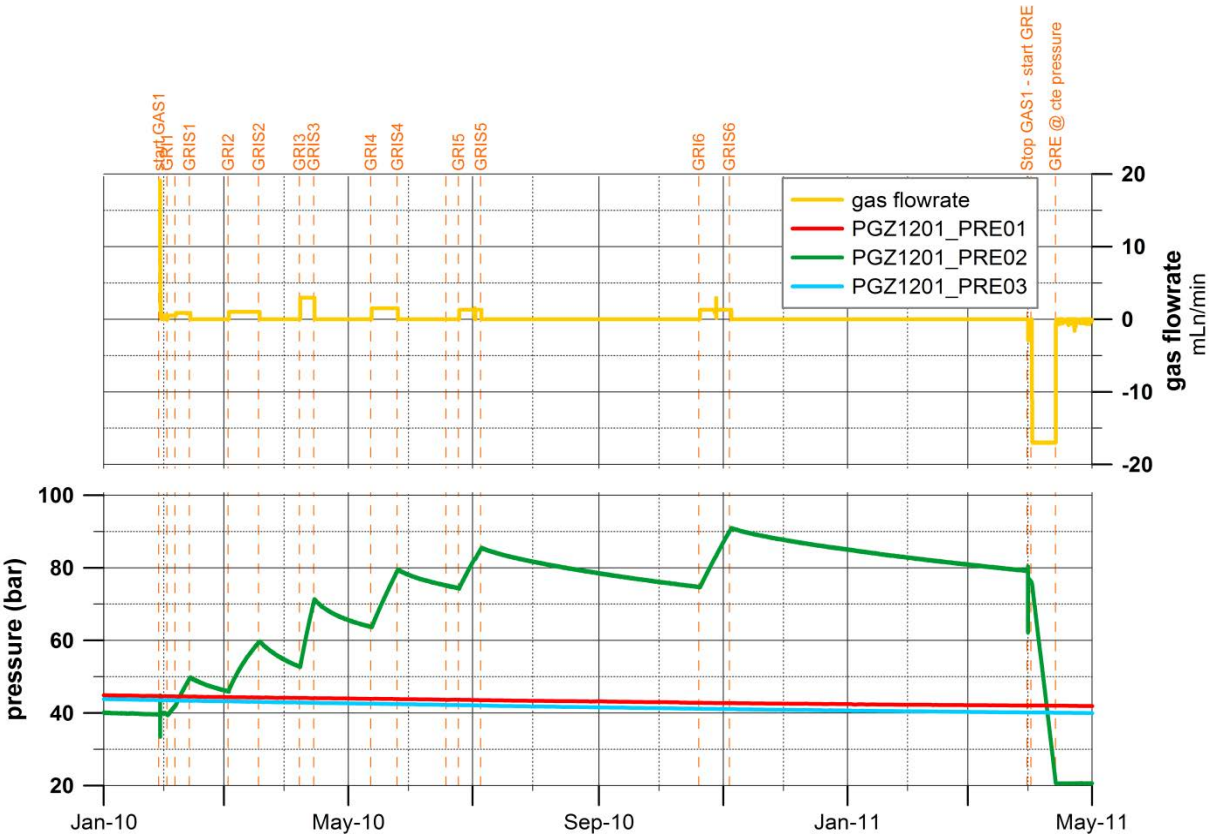

Figure 20 *Pressure and gas flowrate measurements in PGZ1201 from January 2010 to April 2011*

At this scale, there does not seem to be measurable hydraulic interference at Intervals 1 and 3 of borehole PGZ1201, located at 1.69 m from the injection interval.

Zooming in on the measurements for these two intervals (Figure 21) does not demonstrate hydraulic interference either. On this graph, the dotted lines show the linear trend extrapolated from the measurements taken prior to starting gas injection. The curves show a clear tendency to deviate from these lines. Now, it has been demonstrated that the drainage phenomenon associated with borehole PGZ1031 leads to a pressure reduction that dampens over time (see Figure 14).

Thus, it is difficult to discern the hydraulic interference of this effect.

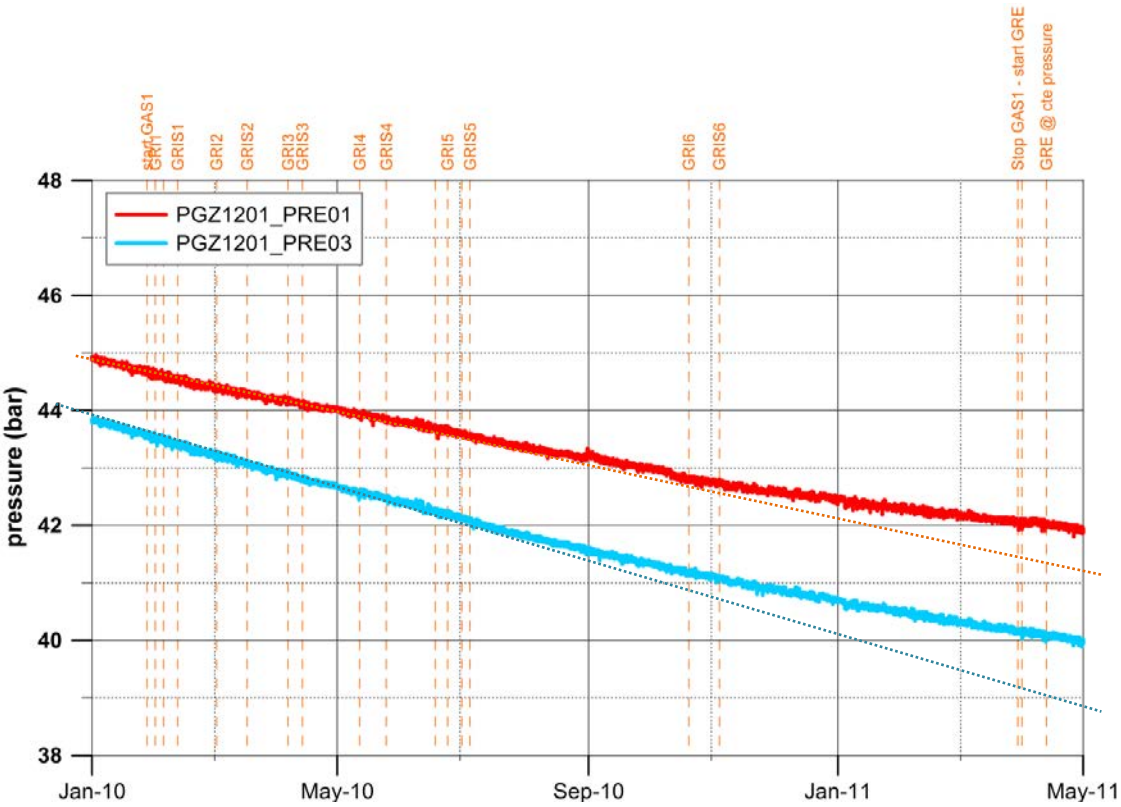

Figure 21 *Detail of the pressure measurements for Intervals 1 and 3 of PGZ1201 from January 2010 to April 2011*

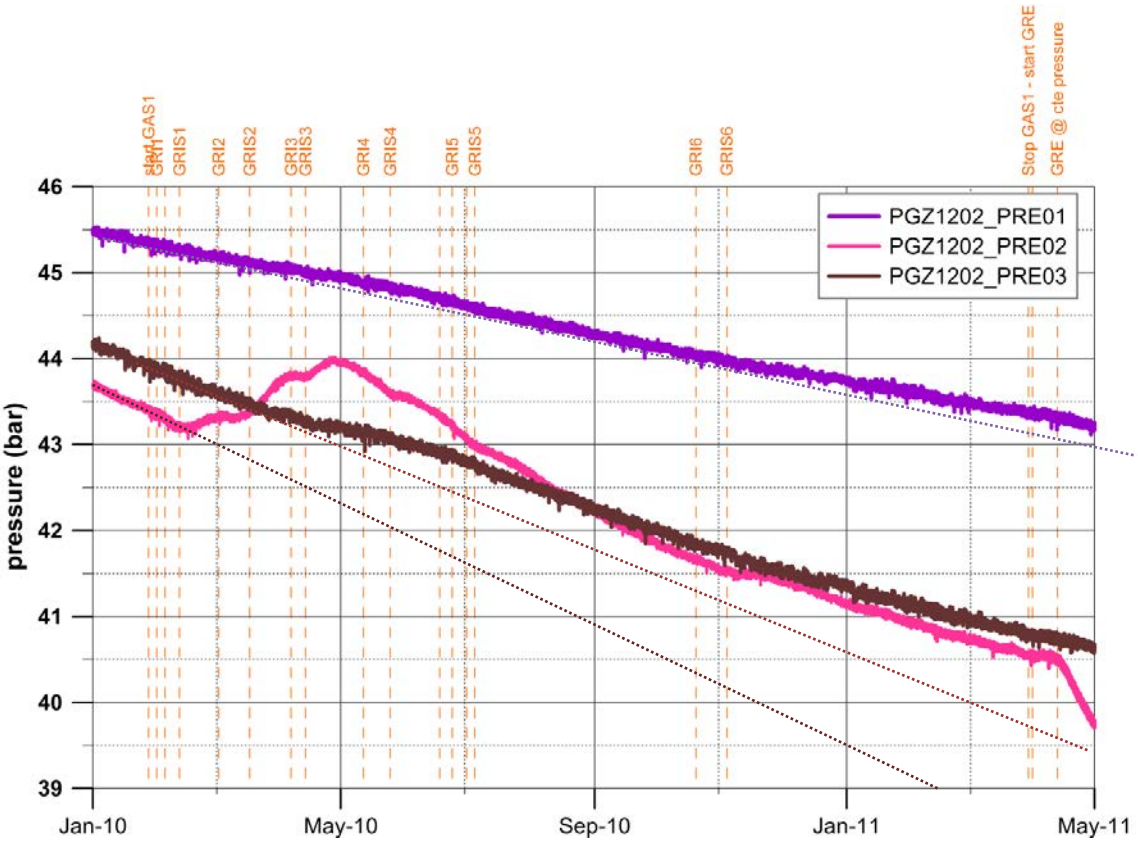

Figure 22 *Pressure measurements in PGZ1202 from January 2010 to April 2011*

Figure 22 shows the pressure measurements at the three measurement intervals in PGZ1202 between January 2010 and May 2011. As on the graph above, the dotted lines show the linear trend extrapolated from the measurements taken prior to starting gas injection.

For this borehole, the hydraulic interference associated with the gas injection steps is clearly visible at Interval 2 and to a lesser extent at the other two intervals.

At Interval 2, the first three injection steps (GRI1 to GRI3) produced clear hydraulic interference in terms of amplitudes, whereas the following injection steps (GRI4 to GRI6) only produced slight interference. This observation demonstrates a change in the behaviour of the system comprised of the boreholes and the formation.

The "Interval 2"s of PGZ1201 and PGZ1202 are 90 cm apart (wall to wall) and hydraulic diffusivity of the formation can be deduced from the phase lag between the points of inflection for this interference. This hydraulic diffusivity is between $4x10^{-7}$ m²/s and $2x10^{-6}$ m²/s, and by assuming a specific storage[4] of $3x10^{-6}$ m^{-1}, a hydraulic conductivity of between $1.2x10^{-12}$ m/s and $6x10^{-12}$ m/s can be deduced. This range of values is greater than that which was estimated during initial tests without gas (Table 5). The uncertainties associated with the points of inflexion method mean that it is not possible to demonstrate changes in hydraulic diffusivity as gas injection proceeds.

Considering the two monitoring intervals on PGZ1201, which are 1.69 m from the gas injection interval, and assuming a hydraulic diffusivity of 10^{-5} m²/s (for EDZ) or 10^{-7} m²/s (for undisturbed argillite), hydraulic interference would occur after 3.3 days or 330 days respectively. The timescale in Figure 21 covers this period and the *in situ* measurements should, therefore, be influenced by hydraulic interference.

It should be remembered that the hydraulic diffusivity (D in m²/s) is equal to the hydraulic conductivity (K in m/s) divided by the specific storage (Ss in m^{-1}). For values typically encountered in argillite, this gives:

- for a value of 10^{-7} m²/s (undisturbed argillite), this gives two ordered pairs (K/Ss): $10^{-13}/10^{-6}$ or $10^{-12}/10^{-5}$
- for a value of 10^{-5} m²/s (EDZ), this gives two ordered pairs (K/Ss): $10^{-11}/10^{-6}$ or $10^{-10}/10^{-5}$

6.1.2 Packer pressure

Figure 23 shows the pressure measurements for the packers around Interval 2 of PGZ1201, and the pressure measured in Interval 2 from January 2010 to May 2011. The measurement PPK01 corresponds to the pressure measurement for the packer located at the lower end of Interval 2 while measurement PPK02 corresponds to the one located at the upper end.

Packer PPK02 was re-inflated with water on the 18 June 2010 to maintain a minimum pressure difference of 5 bar between the gas pressure in the interval and the packer.

The behaviour of the two packers was very similar during steps GRI1 to GRI3. Next, the behaviour of the packers remained similar during the gas injection phases (GRI4, GRI5 and GRI6) but was different during the pressure-recovery phases where injection into the interval was stopped (GRIS3, GRIS4, GRIS5 and GRIS6). Indeed, the pressure continued to rise in the packer located below the interval (PPK01) and stabilised in the packer located above the interval (PPK02).

This difference in the behaviour of the two packers from GRIS3 onwards demonstrates a change in the behaviour of the system. This point is analysed in Section 7.2.

[4] This specific storage is assumed constant over the whole thickness of the argillite that separates the two boreholes, with no disturbed zones around each borehole.

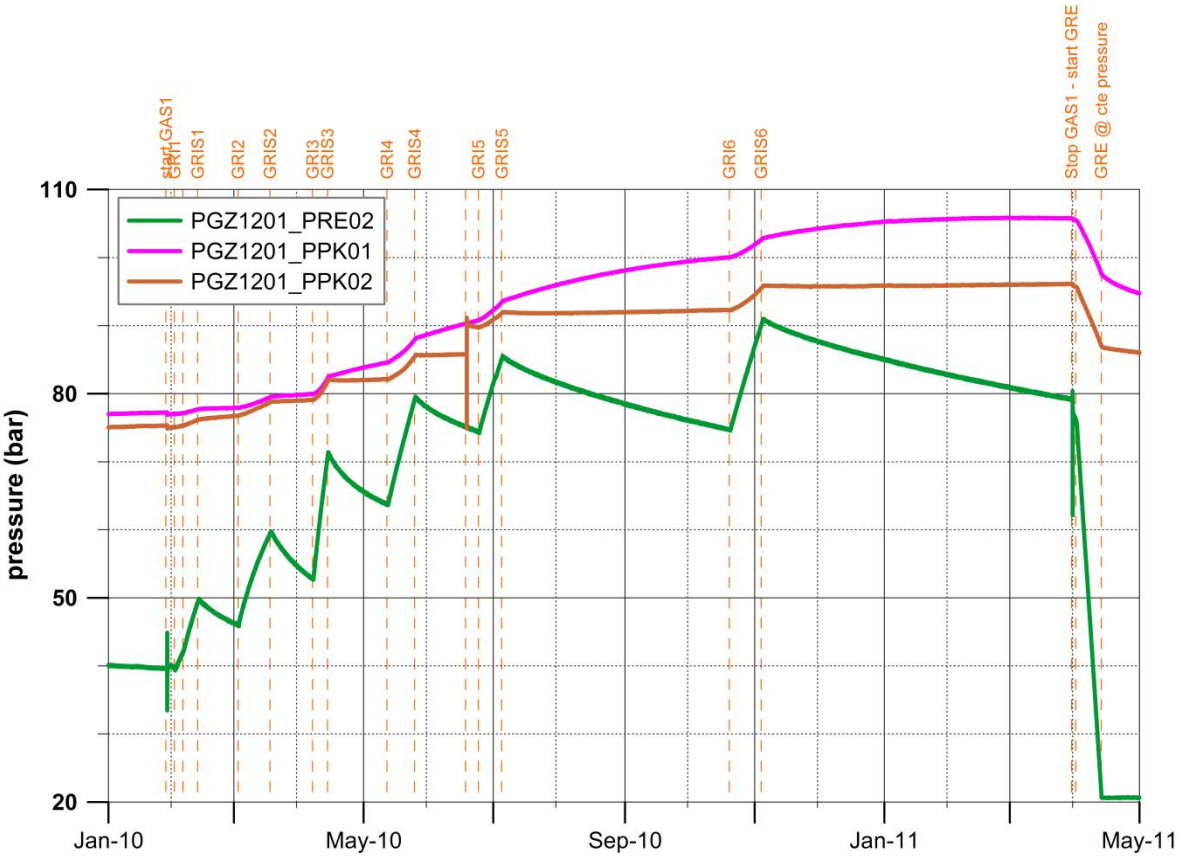

Figure 23 *Comparison of the packer pressure measurements and gas-injection interval pressure (PGZ1201) from January 2010 and April 2011*

6.2 GRIx injection steps

Figure 24 shows the pressure measurements in the injection interval, the gas flowrate and the quantity of gas injected. The flowrate data shows that:

- during the first GRI1 step, the gas flowrate was increased to reach a pressure of 50 bar after 10 days,
- there were two short interruptions in injection due to a problem on the flowmeter during steps GRI5 and GRI6 (too low a pressure difference across the flowmeter).

The quantity of gas injected (in moles) was calculated from data supplied by the flowmeter[5] using the ideal gas law. This provides the cumulative quantity of gas injected.

[5] The flowmeter measurements are given for standard temperature and pressure conditions, i.e. 273.15 K and 101,325 Pa.

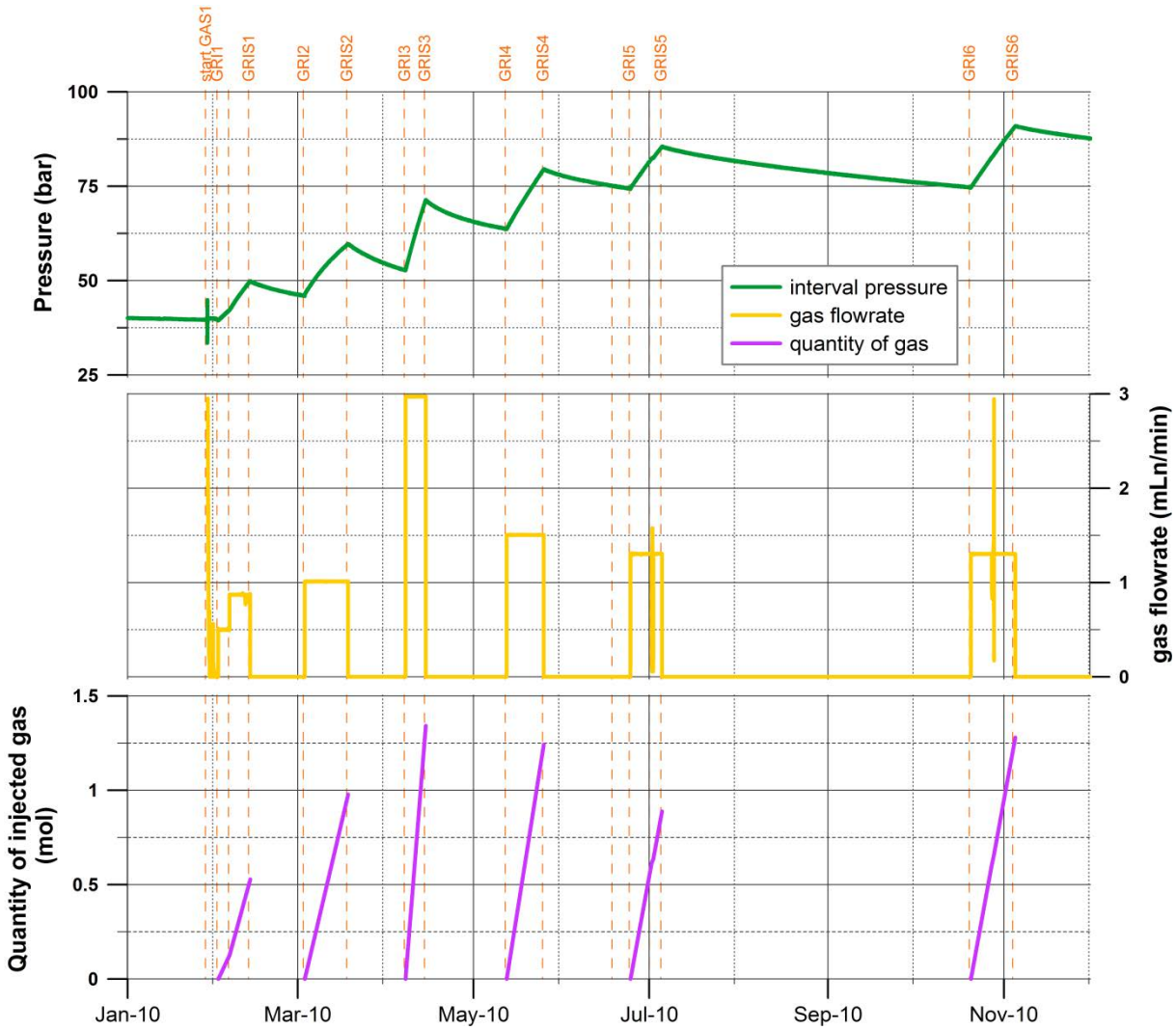

Figure 24 *Flowrate and cumulative quantity of gas injected and pressure measured in Interval 2 of PGZ1201 during GAS1*

The gas injection steps were at increasing pressure levels (see Table 7) but the initial pressure of step GRI_{i+1} was always lower than the final pressure of the preceding step GRI_i due to the fact that pressure recovery phases (GRISx) followed each injection phase.

In all the sections that follow, the graphs that show the pressure measurements or pressure differences have not been corrected for the drainage effect induced by borehole PGZ1031 (see Section 4.2.2) and for dissolution and diffusion of nitrogen in water. It is assumed that the two phenomena (drainage vs dissolution/diffusion) compensate each other.

6.2.1 Comparison of the pressure differences

Figure 25 provides a comparison on a single graph of the pressure difference produced by gas injection as a function of elapsed time for the six injection steps GRI1 to GRI6 adjusted for a normalised gas injection flowrate of 1 ml_n/min (as an example). For this, the pressure difference measurements were multiplied by a coefficient of 1/*injection flowrate.*

The significance of the graph is as follows: the lower the pressure difference per unit time, the better the formation can dissipate the overpressure produced.

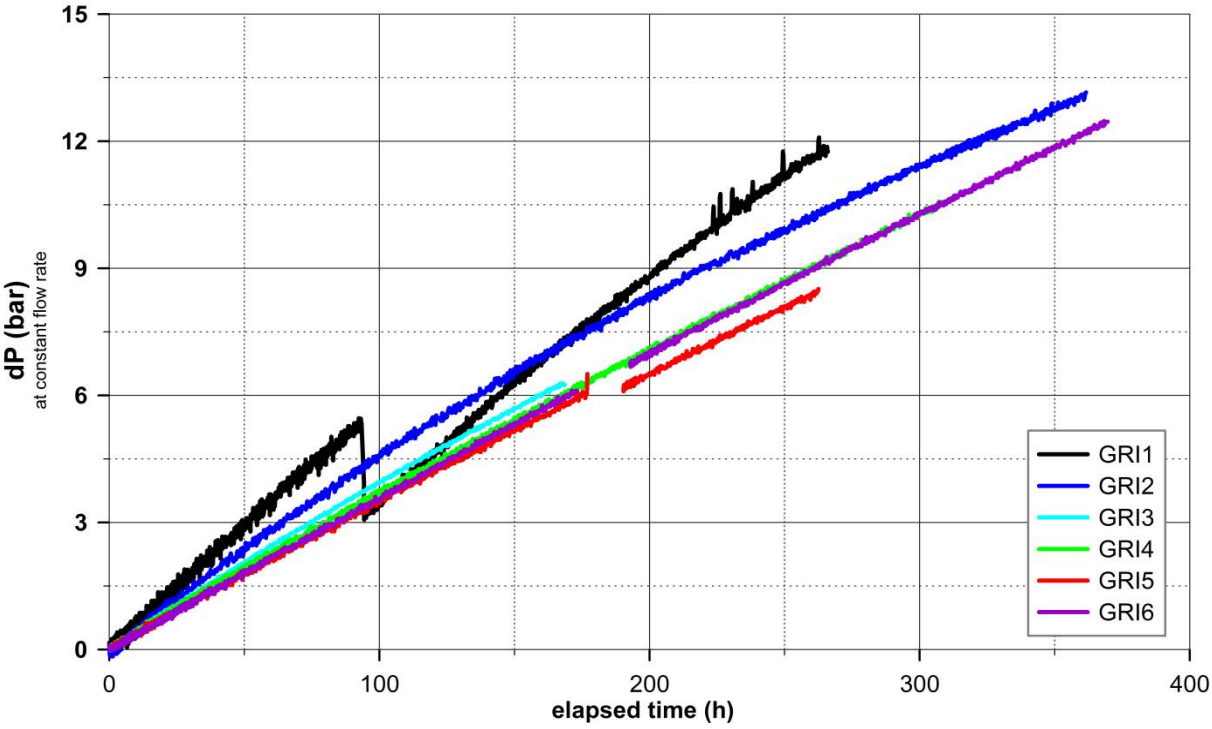

Figure 25 *Pressure difference measured for the six injection steps GRI1 to GRI6 adjusted for a normalised gas flowrate of 1 ml_n/min*

Changes in the pressure difference are fairly uniform for steps 3 to 6, which demonstrates a narrow range of diffusivity values. The distribution is as expected for the standard two-phase model, i.e. no change in the permeability[6] below the pathway dilation threshold. However, there are inconsistencies in detail between the pressure differences for GRI3 and GRI6 combined and GRI5 which shows a higher permeability.

If the gas pressure had exceeded the pathway dilation threshold, a reduction in pressure difference over time would be expected to have been observed.

As stated in Section 5.3, the measured gas pressures result from the combination of a constant-volume compression effect and from a change in system volume. Only the change in volume provides information on changes in the formation's diffusivity.

6.2.1.1 Analysis of the pressure differences as measured and as calculated at constant volume

In Figure 26, the method given in Section 5.3 has been applied. For each injection step (GRI1 to GRI6), the following are shown: the measured pressure difference and the calculated pressure difference assuming a constant volume for the interval for the two extreme cases 804 cm^3 and 1540 cm^3 which correspond to the theoretical minimum and maximum volumes of Interval 2 of PGZ1201 (see Section 4.2). The pink curves correspond to the calculated pressure difference at the constant volume that gives the best fit to the measurements.

[6] To the extent that specific storage remains constant

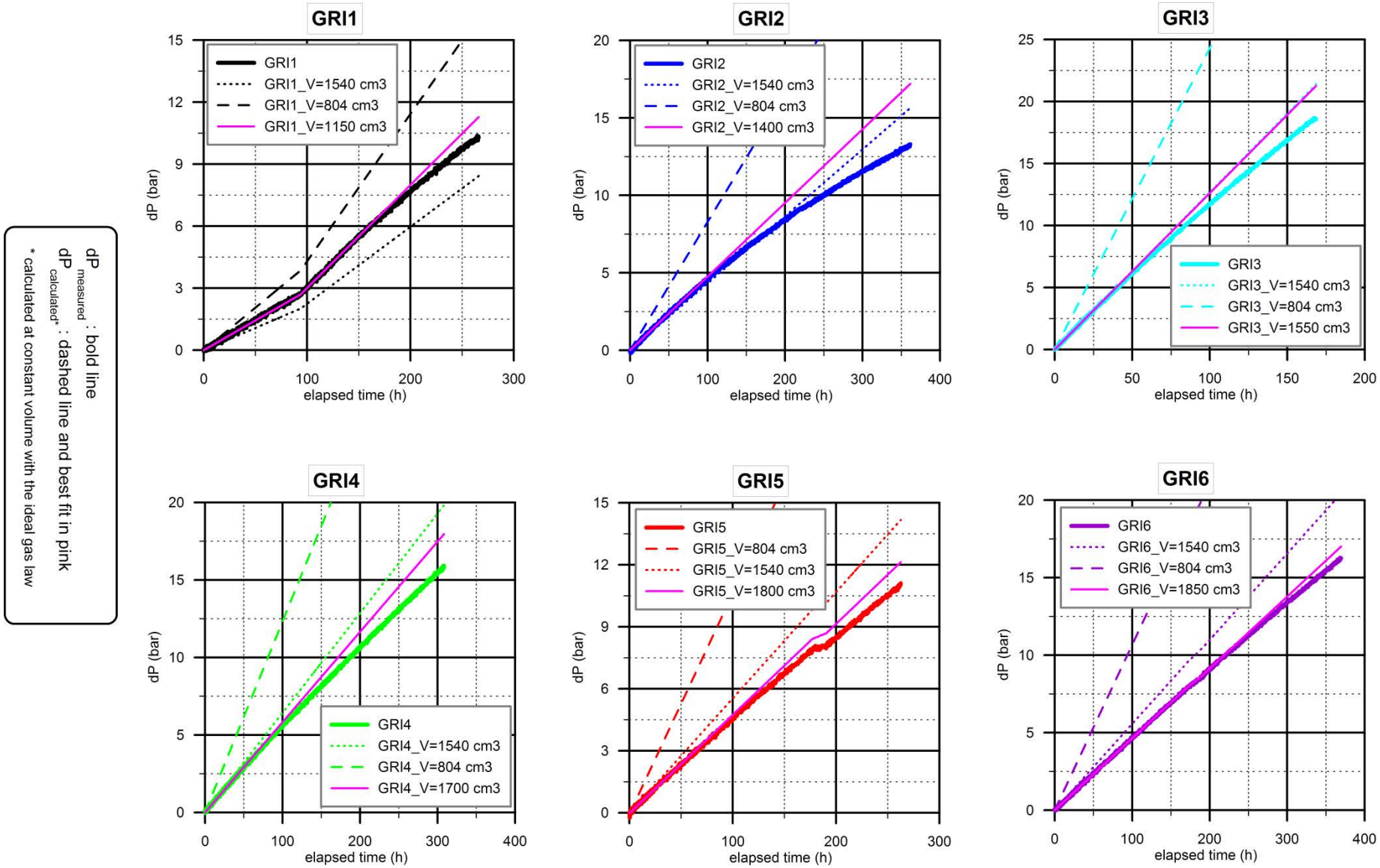

Figure 26 *Comparison of the pressure difference as measured and as calculated at constant volume for the six steps GRI1 to GRI6*

6.2.1.2 GRI1

The measured pressure difference is clearly between the pressure differences calculated for the extreme volumes. At the start of the step, the best fit corresponds to a volume of 1150 cm^3, i.e. a volume larger than that calculated during the water extraction phase (1040 cm^3, see Section 5.3). This result is interpreted as being due to movement of water from the interval into the rock during the short constant pressure step.

The measured pressure difference only significantly deviates from the calculated best-fit pressure difference after approximately 200 hours (i.e. 8.3 days). This means that during these first two hundred hours, the gas volume remained constant (compression effect) and that only after this did the interval volume available for the gas increase.

In the standard two-phase model, where the relative permeability of water is much higher than the permeability of gas above 90% saturation, and from the fact that there was residual water in the test interval, it is clearly this residual water that is moved and pushed into the argillite.

Going back to the previous period, i.e. the water-extraction phase where the gas volume increased by 110 cm^3 (see Section 5.3), the question could be asked as to what physical phenomenon produced this change in volume by water displacement. This could either be a pressure gradient between the filter and the rock, which would be explained by a historical effect or unstabilised thermal equilibrium, or a slight desaturation of the borehole wall by the various gas flushings followed by imbibition of the free water contained in the interval. This last hypothesis would indicate a very low gas entry pressure of just a few bar.

6.2.1.3 GRI2

At the start of the step, the best fit corresponds to a volume of 1400 cm^3. This shows that during GRI1 and GRIS1, there was in increase of nearly 250 cm^3 in the volume available for the gas, which is equivalent to the expulsion of residual water from the test interval into the argillite.

The measured pressure difference only significantly deviates from the calculated best-fit pressure difference after approximately 100 hours (i.e. 4.1 days). During these first hundred hours, the gas volume remains constant (compression effect) and only afterwards does the interval volume available for the gas increase by expelling the residual water.

Given the above, slight gas penetration into the formation cannot be excluded, in parallel with water expulsion into the rock which remains the dominant phenomenon.

6.2.1.4 GRI3

The best fit corresponds to a volume of 1550 cm^3. This shows that during GRI2 and GRIS2, there was an increase of nearly 150 cm^3 in the volume available for the gas.

The best-fit volume is almost identical to the maximum theoretical volume of Interval 2. Furthermore, during the first fifty hours, the measured pressure difference follows the calculated pressure difference for constant volume and, beyond this, the volume of the gas increases.

Thus, during steps GRI2, GRIS2 and the first fifty hours of GRI3, the remaining residual water is expelled from the interval and only after this does the gas starts to penetrate into the rock.

The interval gas pressure is of the order of 58 bar, which corresponds to a gas entry pressure of approximately 20 bar given that the water pressure is estimated at 38 bar (see Figure 6). This value is a maximum value as it depends both on the volume of residual water in interval and, probably, on the injection kinetics. For example, less residual water would lead to earlier gas penetration and, thus, a lower gas entry pressure.

6.2.1.5 GRI4 – GRI5 – GRI6

For these last three gas injection steps, the gas volume estimated by the best fits is always greater than the maximum theoretical volume of Interval 2. It is certain therefore that, after GRI3, there is no residual water in the injection interval.

The increase in gas volume at the start of these three steps reduces from 100 cm^3 between steps GRI4 and GRI5 to 50 cm^3 between GRI5 and GRI6.

Thus, the gas finds it increasingly difficult to penetrate the rock as the pressure rises. This is also confirmed by considering the discrepancy between the pressure difference calculated for the best fit and the measured pressure difference. This discrepancy does indeed reduce significantly between step GRI4 and step GRI6.

6.2.2 Comparison of the pressure differences without compressibility effects

For each injection step, the discrepancies calculated between the best-fit pressure differences estimated at constant volume and the measured pressure differences give access to the real pressure variation of the gas volume without the gas compression effect.

These calculated discrepancies are still dependent on the gas flowrate injected and, to overcome this, they must be normalised to a constant gas flowrate of 1 ml_n/min. The normalised discrepancies are shown in Figure 27 and have been recalculated by multiplying the discrepancies by a coefficient equal to 1/*injection flowrate.* This graph gives a better representation of the ability of the gas to penetrate the formation around the borehole wall.

The significance of this graph is the opposite of Figure 25; the smaller this discrepancy per unit time, the less the interval volume increases and, thus, the less easily the gas penetrates the formation.

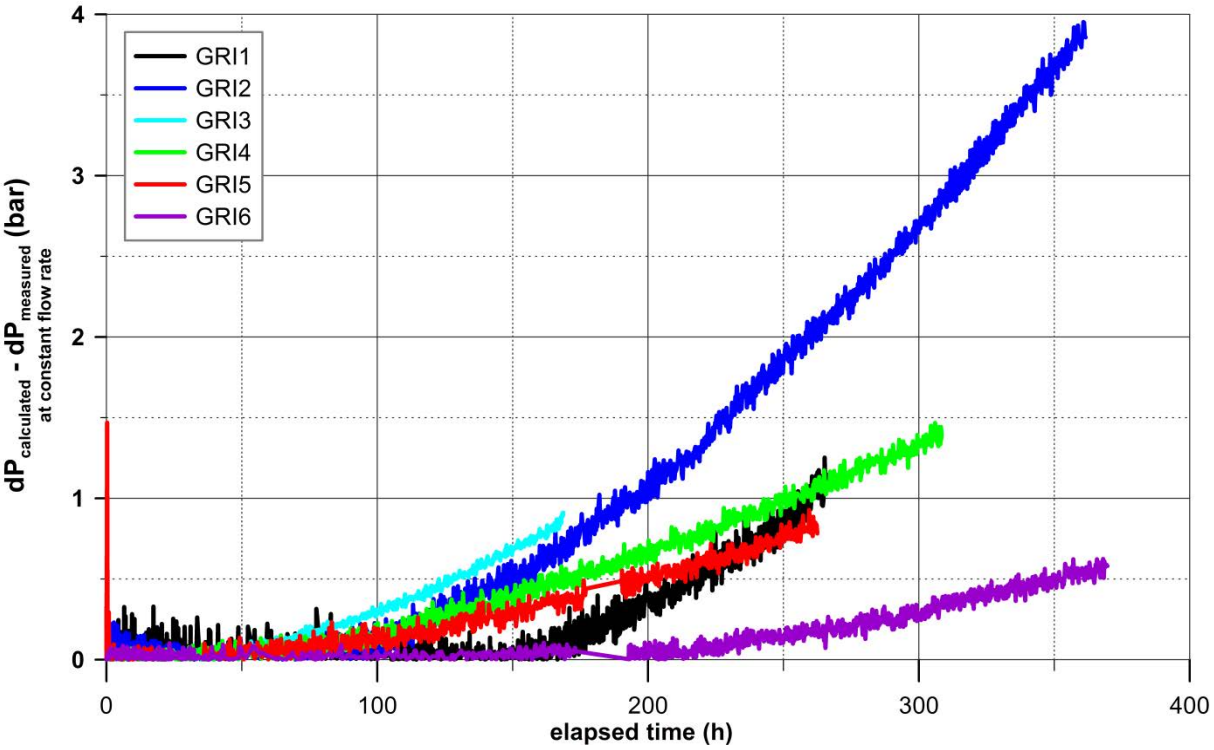

Figure 27 *Pressure discrepancies calculated without the gas compressibility effect, normalised to an injection flowrate of 1 ml_n/min*

As water remained in the injection interval during the first three steps, no change in the ability of the gas to penetrate the formation is observed between GRI1 and GRI3.

Conversely, the normalised discrepancies for steps GRI3 to GRI6 show that the gas is able to penetrate the rock. The reduction in normalised discrepancies for steps GRI4 to GRI6 corresponds to a real reduction in the ability of the gas to penetrate the argillite.

6.3 Comparison of the GRISx pressure recovery steps

6.3.1 Pressure difference

Figure 28 shows the measured pressure differences in Interval 2 of PGZ1201 during the six pressure recovery steps. These curves may be directly compared as there is no gas injection flowrate. The significance of the graph is as follows: the greater the measured pressure difference per unit time (i.e. the steeper the gradient), the faster the overpressure produced in the interval is dissipated.

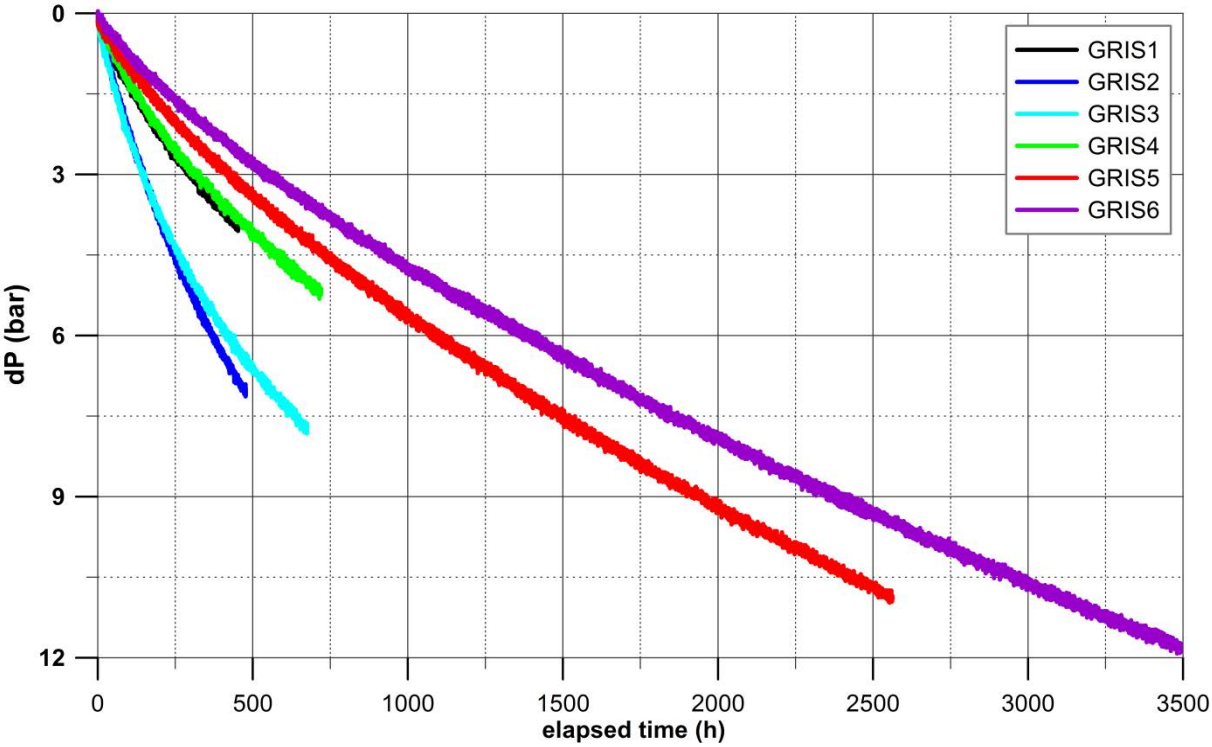

Figure 28 *Pressure difference measured during the pressure recovery steps (GRIS1 to GRIS6)*

In fact, this graph is very similar to Figure 27, which gives flowrate-normalised pressure differences, in that only steps GRIS3 to GRIS6 are representative of the ability of the gas to penetrate the rock due to the fact that, from GRIS3, water has been completely expelled.

The pressure gradient falls between each step. This means that there is a slight reduction in diffusivity around the borehole.

A summary comparison of all GAS1 steps is given in Section 8.

6.3.2 Horner plot

Figure 29 shows these same pressure recovery phases but with the Horner time on the x-axis. This is an inverse time axis of the form $(t_p + dt)/dt$ where t_p corresponds to the time since each injection phase (GRIx) started. Thus, as dt tends to infinity, the Horner time tends to 1.

Each curve tends towards a linear part as it approaches the y-axis. The extrapolation of these linear parts cuts the y-axis at a pressure value called the Horner extrapolated pressure. This pressure is assumed to be the stabilised interstitial pressure after an infinite recovery time.

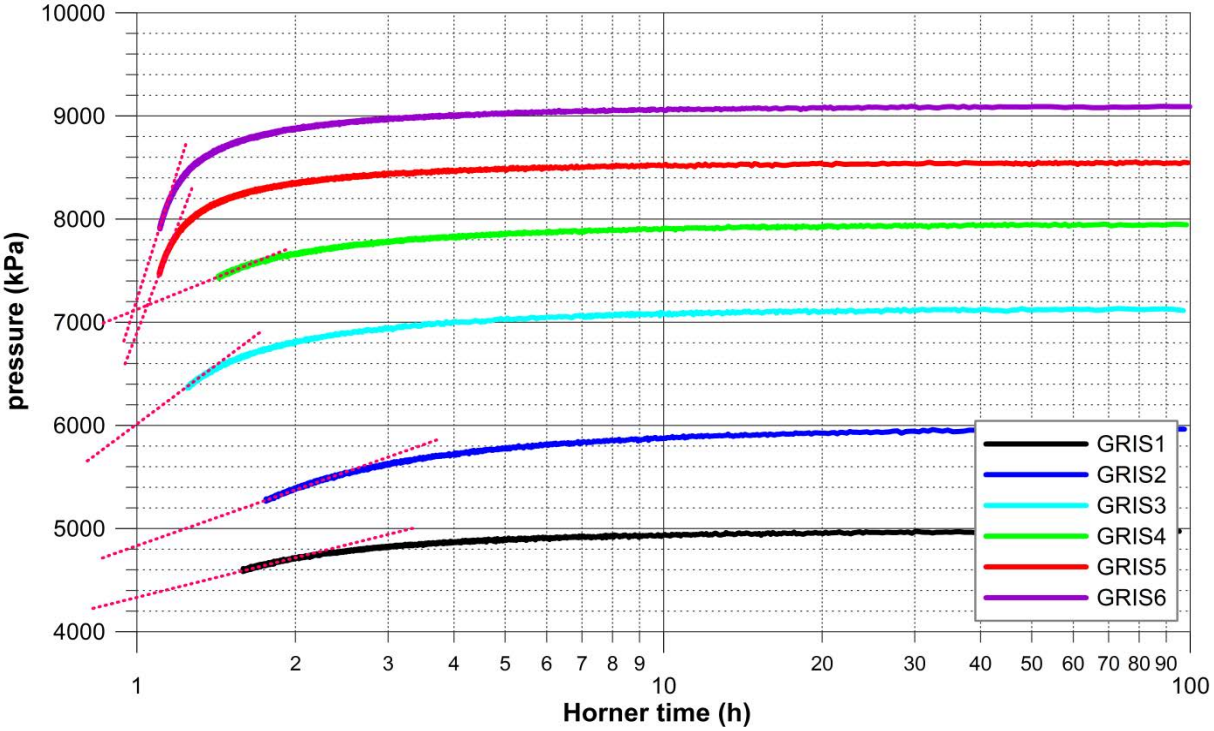

Figure 29 Horner plot for the GRISx steps

The difference between the extrapolated pressure and the stabilised interstitial pressure (fictitious pressure estimated from Figure 6) gives access to the capillary pressure. Thus, between step GRIS2 and step GRIS3, where the gas begins to penetrate the argillite, the capillary pressure is between 10 bar and 22.5 bar. This range agrees with the value deduced from the analysis of pressure differences deduced from the injection phases (see Section 6.2.1.4).

It can be seen that, during the last three pressure recovery steps, the extrapolated pressure is of the order of 70 bar to 72 bar. This capillary pressure seems to increase between GRIS5 and GRIS6 from 34.5 bar to 37.4 bar. This increase suggests gas penetration into smaller diameter pores.

7. Gas extraction and water refilling phase

This phase covers the period from 30 March 2011 to early August 2011. Firstly, the pressure measurements for this whole period are given.

7.1 Pressure measurements

Figure 30 and Figure 31 show the pressure measurements recorded for boreholes PGZ1201 and PGZ1202 respectively, between March 2011 and August 2011. For PGZ1201, the pressure at the two packers, which was continuously monitored, is also given.

It should be noted that during the extraction phase, pressure PGZ1201_PRE02 on Figure 30 is the pressure measured by the pressure sensor located in the gas module (see Appendix 1). This is due to the fact that an extraction system was added between the control panel and the gas module (see Figure 36).

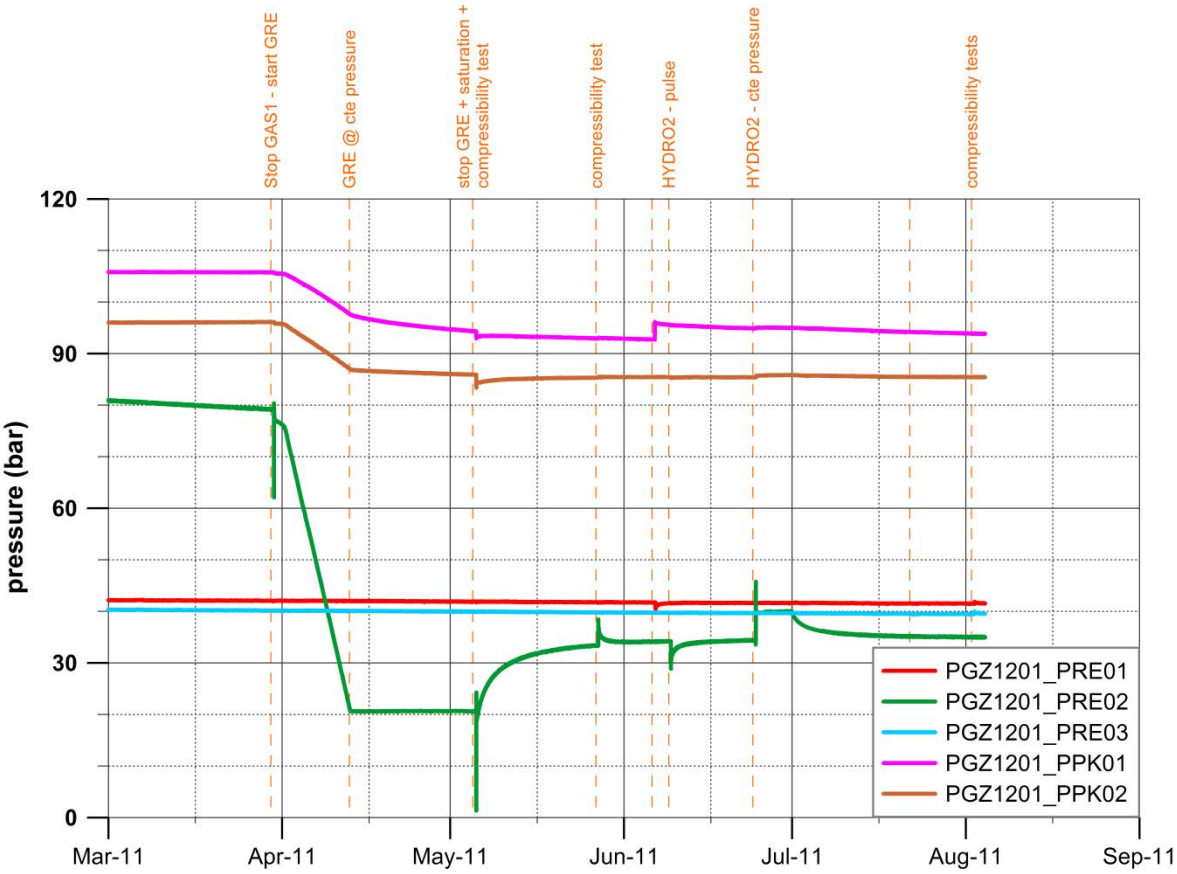

Figure 30 *Pressure measurements for the three intervals and two packers of PGZ1201 during the extraction phase and after refilling with water*

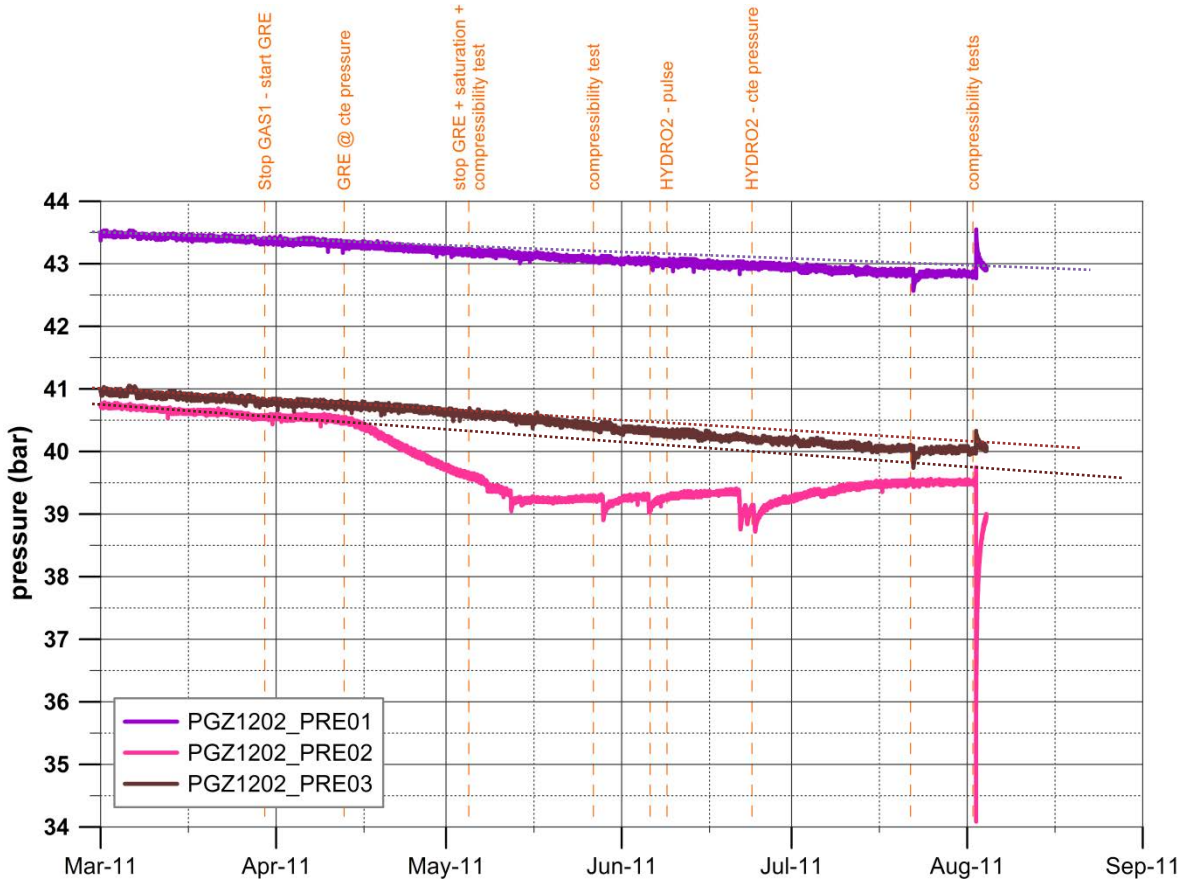

Figure 31 *Pressure measurements for the three intervals of PGZ1202 during the extraction phase and after refilling with water*

The gas extraction phase produced heavy stresses in the rock with a 59 bar reduction in gas pressure at Interval 2 of PGZ1201 over a period of 14 days.

Up to the beginning of August, no interference appeared at the two intervals either side of the loaded interval (Figure 30). In contrast, hydraulic interference is visible at the three intervals of borehole PGZ1202 (Figure 31). The dotted lines correspond to the linear extrapolation of the pressure measurement just before the gas extraction phase started.

The packers reacted to the decompression in the tested interval, with an identical mean gradient (-0.6 bar/day) for the two packers during the constant-flowrate extraction phase and then a slightly different gradient for PPK01 (-0.15 bar/day) and PPK02 (-0.04 bar/day) during the constant-pressure extraction phase. The pressure at PPK01 continued to fall after refilling Interval 2 of PGZ1201 with water, while it stabilised at approximately 85-86 bar for PPK02.

7.2 Hypothesis concerning packer behaviour

The measurements on the packers next to the gas injection interval can be summarised as follows: the series of injection steps caused a hydraulic overpressure in the argillite which diffused along the packers. After the third injection step (GRI3), the gas invaded the rock and caused a distinction between the behaviour of the two packers next to the loaded interval (Figure 32) during the pressure recovery steps (GRIS3, GRIS4, GRIS5 and GRIS6) such that:

- at the lower packer (PPK01) the pressure increased; this damped down, however, over several weeks,
- at the upper packer (PPK02), there was a very small pressure drop followed by stabilisation.

Previously, during the first three pressure recovery steps, the pressures at packers PPK01 and PPK02 had stabilised.

As packer pressure is generally not continuously monitored, there is no experience feedback on packer behaviour under hydraulic loads, even less so for gas loads. Indeed, only the packer measurements for boreholes in the DIR, PGZ1 and PGZ2 tests have been recorded. For boreholes in the DIR experiment, as the interstitial pressure was in equilibrium with the formation, the packers were not affected.

In fact, it is very difficult to know which side the gas would leave along the borehole, as two opposing hypotheses are plausible:

1. The packer experiences the effective stress and the associated strains,
2. The packer experiences both the stress and the interstitial pressure, and the associated strains.

If the fluid producing the overpressure is water then, in the first hypothesis, the overpressure produced in the interval reduces the effective strain. The pressure in the packer should reduce.

In the second hypothesis, the overpressure produced in the interval increases the pressure in the packer. However, there is competition between what the packer directly experiences via surface contact with the interval and the propagation of the overpressure along the surface of the packer.

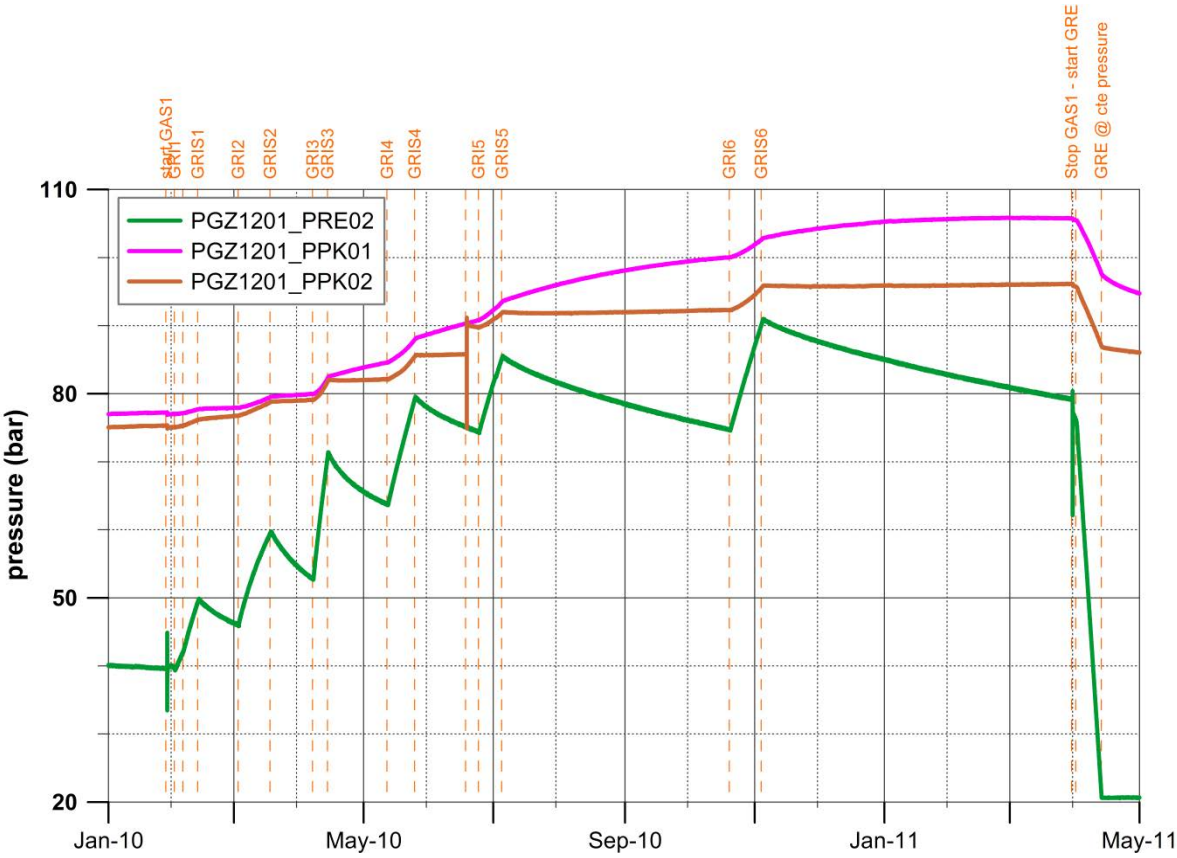

Figure 32 *Comparison of the packer pressure measurements and gas-injection interval pressure (PGZ1201) from January 2010 and April 2011*

Figure 33 gives a simplified, schematic diagram of the propagation of the overpressure along the packer during a pressure recovery step. Depending on the speed of overpressure propagation, the proportion of surfaces under overpressure (position of the overpressure peak) can lead to three possible diagrams (corresponding to increase, stabilisation and reduction of pressure in the packer).

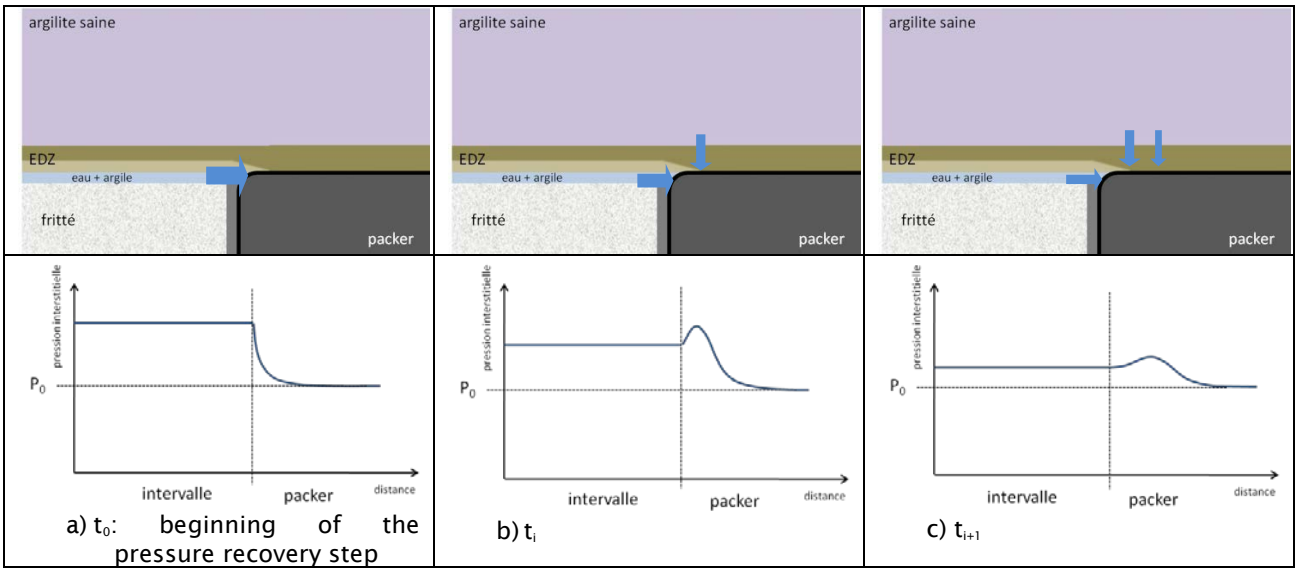

Figure 33 *Propagation of the overpressure along a packer during a pressure recovery phase*In the current case, the propagation of the overpressure seems to have produced pressure stabilisation in both packers.

Thus, it seems that the packer experiences both the stress and the interstitial pressure (hypothesis 2), providing there is no strain elsewhere. Hypothesis 2 is supported by the monitoring of packer pressure in the other boreholes, where it is seen that the packer pressure follows the interstitial pressure (for example PGZ1013, Figure 34).

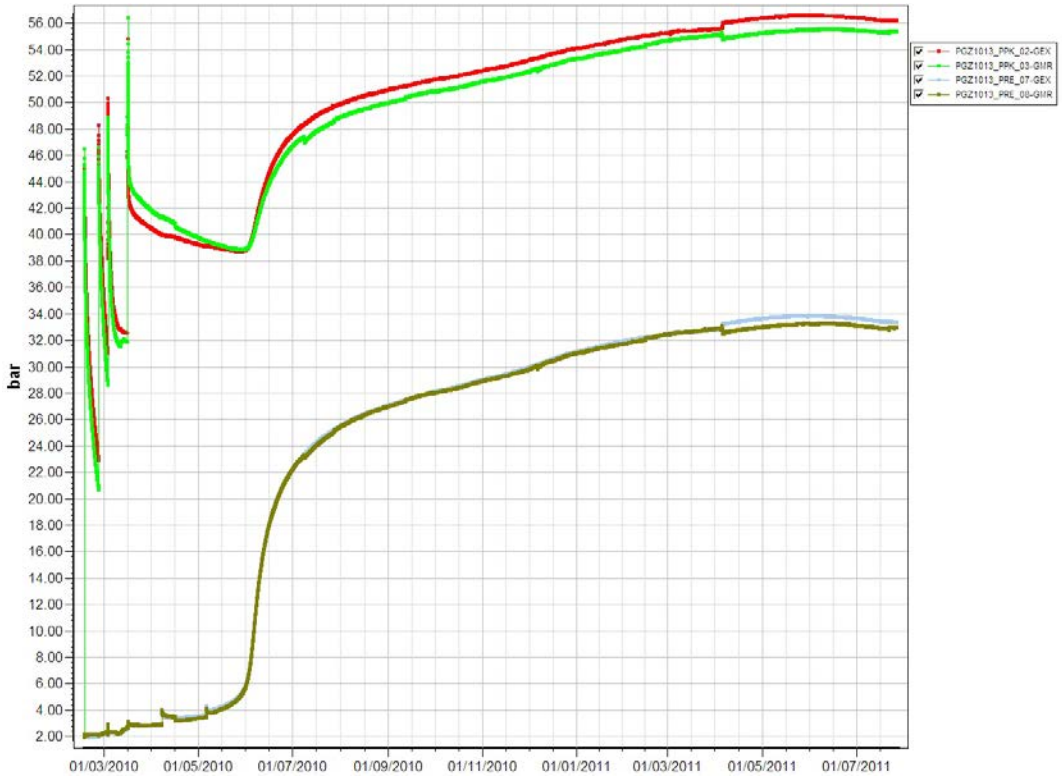

Figure 34 *Monitoring interstitial pressure (red, green) and pressure in PGZ1013 packers (blue, khaki)*

This becomes more complex when the overpressure is produced by gas, which is compressible.

Indeed, from a hydraulics standpoint, the fact of injecting gas into the rock will change the saturation and, thus, the specific storage. The specific storage equation is as follows (Freeze A.F. and Cherry J.A., 1979):

$$Ss = \rho . g . (\alpha + n . \beta)$$

Where:

- ρ = density of water [kg/m^3],
- g = gravitational acceleration [m/s^2],
- α = compressibility of the rock grains [Pa^{-1}],
- n = porosity [-],
- β = compressibility of water [Pa^{-1}].

In a partially saturated formation, the compressibility of water can be expressed by the following equation (Schanz T., 2003):

$$\beta = \beta_0 + \frac{(1 - S)}{P_a + p}$$

Where:

- β_0 = compressibility of reference water [Pa^{-1}],
- S = saturation [-],
- P_a = atmospheric pressure [Pa],
- p = pore pressure [Pa].

The specific storage as a function of saturation can be calculated by combining these two equations (see Figure 35).

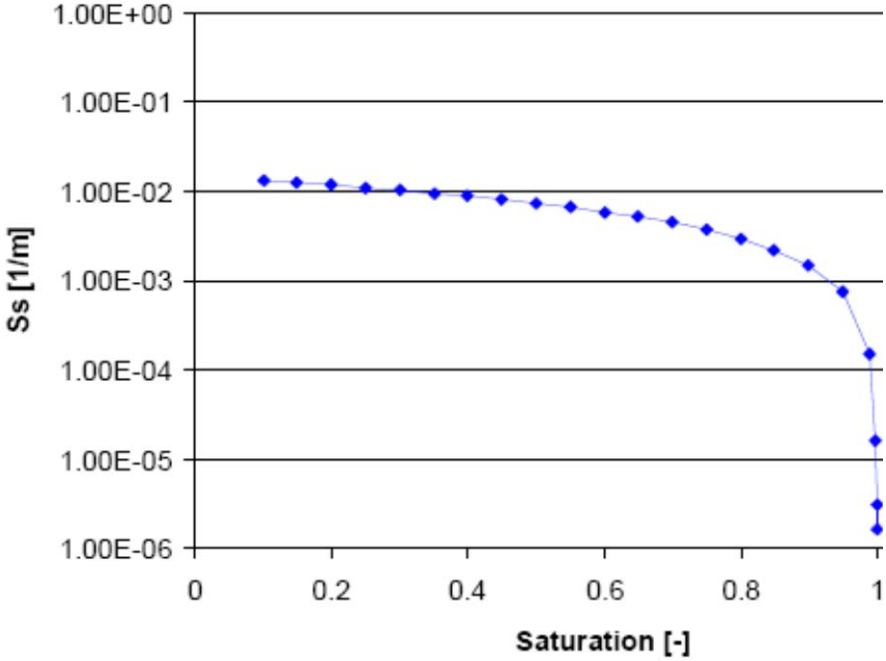

Figure 35 Specific storage as a function of saturation

It can be seen that there is a very large increase in specific storage for a small desaturation. For example, 5% desaturation leads to the specific storage rising from ~$2x10^{-6}$ m^{-1} to ~$8x10^{-4}$ m^{-1}.

By injecting gas into the rock, the specific storage is greatly increased, which leads to a drop in diffusivity[7]; this means that the speed of propagation of the overpressure along the packer is reduced.

Thus, to explain the behaviour of packer PPK01, the gas preferentially travelled slowly along the packer below the test interval. Furthermore, the superposition of gas injection steps may have led to an accumulation of gas and a larger desaturation below the injection interval. This process further slowed the propagation of the overpressure.

What remains to be explained is why the gas travelled downwards rather than upwards along the borehole. It should be remembered that draining borehole PGZ1031 passes perpendicularly and obliquely above borehole PGZ1201 (see Figure 3). Now, the vertical plane that passes through borehole PGZ1031 cuts borehole PGZ1201 at lower packer PPK01 at 14cm from the edge of Interval 2 of PGZ1201 (distance in a horizontal plane). Thus, the gas followed the decreasing pressure gradient along the borehole.

To confirm the hypothesis suggested above, a poro-mechanical analysis should be performed to understand the impact of gas injection on the strains and interstitial pressure around the packers.

7.3 Gas extraction phase (GRE)

7.3.1 Purpose, preparation and implementation

The purpose of this phase was to extract the maximum quantity of gas over a period of approximately 30 days so that, after resaturation, a hydraulic test could be performed in conditions similar to those of test HYDRO1.

This extraction phase was designed by AF CONSULT - INTERA – Intera (D.RP.0CPE.11.0004). The procedure adopted for this phase was to extract gas first at constant flowrate then at constant pressure.

For this extraction phase, a chamber on a weighing scale and a pressure measurement column were added between the gas module and the control panel for borehole PGZ1201 (see Figure 36). The chamber and column were to allow any water that may be extracted from Interval 2 to be collected and measured.

[7] The effective permeability (i.e. of the gas and water phases together), remains essentially constant until saturation drops to 80%.

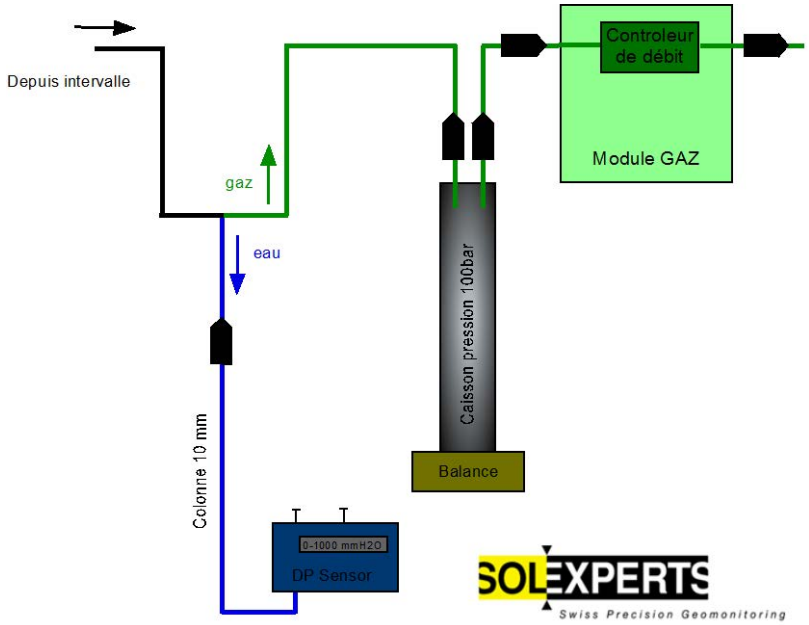

Figure 36 Schematic diagram of the extraction system

The volumes added are given in Appendix 3. Before the extraction phase started, this additional volume of 4144 cm^3 was filled with gas at a pressure almost identical to that of Interval 2. The volume added corresponded to 13.3 moles of nitrogen.

The gas extraction phase was started on 30 March 2011 and completed on 5 May 2011. It was therefore performed over a period of 36 days (see Table 2), under the following conditions:

- constant flowrate of 2.9 ml_n/min for 2 days (connected to the small flowmeter $V_{extraction}$ = 4144 cm^3),
- a flowrate of 16.9 ml_n/min for 12 days (connected to the medium flowmeter $V_{extraction}$ = 4130 cm^3),
- constant pressure of 20 bar for 22 days (connected to the small flowmeter $V_{extraction}$ = 4144 cm^3).

7.3.2 Extraction flowrate

Figure 37 shows the pressure measurement in Interval 2, the gas flowrate and the cumulative quantity of gas extracted (calculated using the ideal gas law). The flowrate and quantity are negative to show that this concerns extraction of gas from the interval and the rock into the drift.

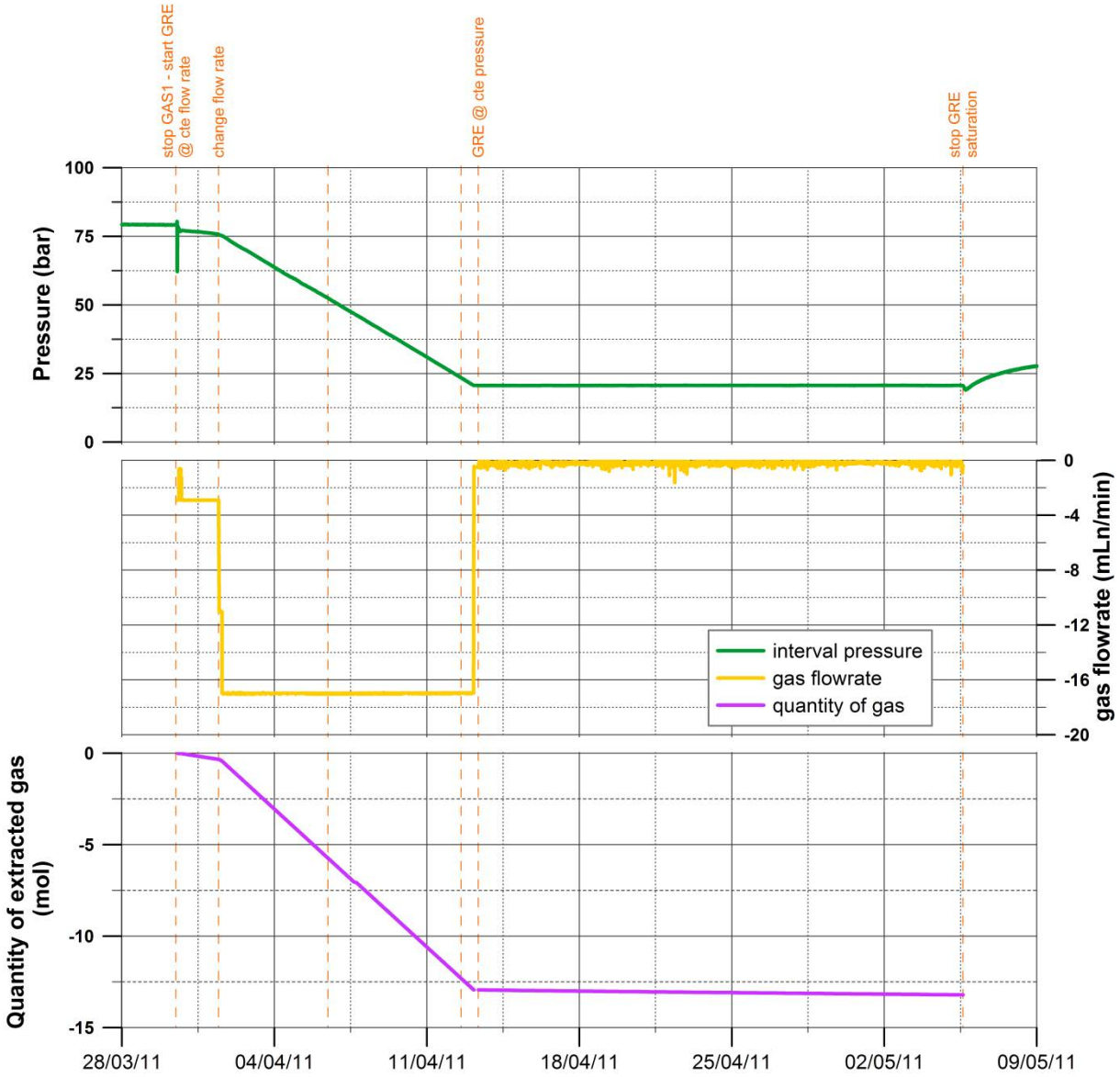

Figure 37 *Flowrate and cumulative quantity of gas extracted, and pressure measured in Interval 2 of PGZ1201 during the GRE phase*

The quantity of gas extracted during this phase was 13.2 moles.

The water collection systems (chamber and column) did not collect any water from the interval.

7.3.3 Analysis of the pressure difference as measured and as calculated at constant volume

In Figure 38, the method given in Sections 5.3 and 0 has been applied. The three graphs give the pressure difference as measured and as calculated using the ideal gas law for the gas extraction phase (first two graphs at constant extraction flowrate and last graph at constant pressure).

The volume under consideration corresponds to the test interval (volumes V_1, V_2 and V_3 from Figure 18), a certain volume of gas that has penetrated the argillite and the volume of the extraction system in the drift (see Appendix 3).

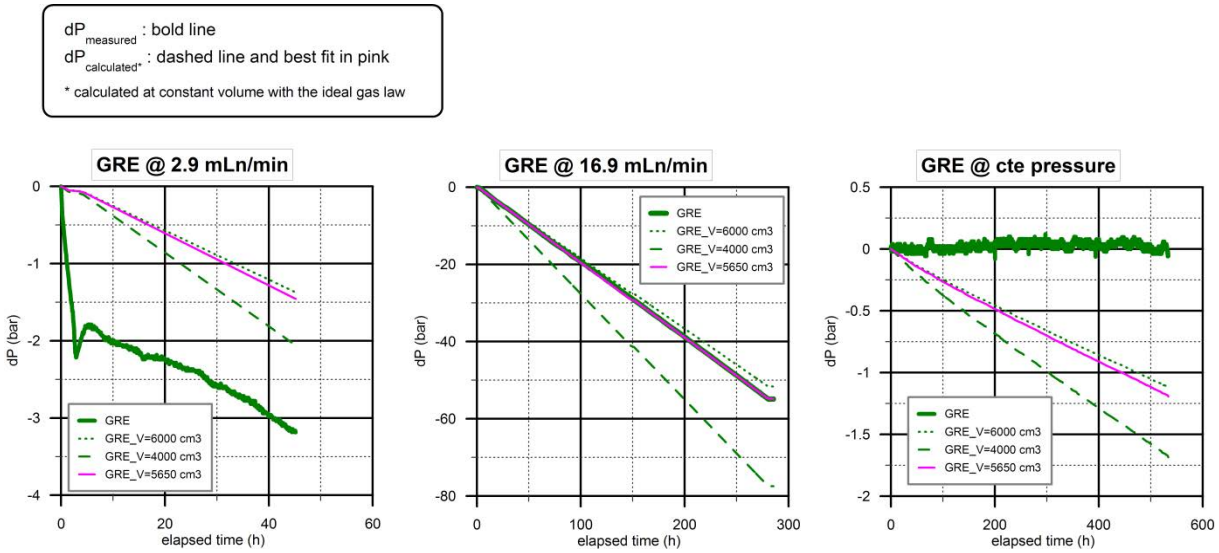

Figure 38 *Comparison of the pressure difference as measured and as calculated at constant volume for the extraction phase*

- The first period (left graph) shows that the pressure difference calculated for two different extreme volumes (4000 or 6000 cm³) does not give a good fit to the measured pressure difference. After the first 10 hours, the pink curve, which corresponds to a volume of 5650 cm³, has the same gradient as measured pressure. The first period of the extraction phase could not be reproduced by the simple decompression of the gas in a container of constant volume.
  - ✓ This could be due to a phase where the pressures and temperature of the two containers – the interval and the extraction system in the drift – reach equilibrium.
- The second period (middle graph) shows that the pressure difference measured could be exactly reproduced by simple gas decompression in a container with a constant volume of 5650 cm³. Thus, there is no movement of fluid from the argillite into the test interval during this period.
- The third period (right graph) shows that it is not possible to reproduce the pressure difference measurement by a simple decompression of gas in a container of constant volume.
  - ✓ The arrival of fluid (water or gas) into the test interval compensated for the gas extracted by the flowmeter.
    - If only gas is considered, this would tend to indicate that a certain volume of gas injected into the argillite during the GAS1 phase was no longer part of the gas volume in this reservoir during the extraction phase. There would, therefore, be a discontinuity in the gas phase in the argillite. However, this gas phase trapped in the argillite would be easily displaced.
    - If water is considered, the gas volume would tend to reduce little by little. Water ingress would occur in the interval.

7.4 Refilling with water

Interval 2 of PGZ1201 was refilled with water on 5 May 2011. After the extraction system was disconnected, the pressure was again measured via the sensor linked to the interval.

The procedure used was as follows:

i. Open the interval valve on the control panel, allowing remaining gas to escape first naturally and then using a vacuum pump; this lasted 14 minutes,

ii. A series of CO_2 injections followed by vacuum for 5 minutes,

iii. Saturation of the interval. **Volume of water injected: 1119 cm³**,
   - This volume is significantly lower than the maximum theoretical volume ($V_{int2\ max}$ equal to 1540 cm³), which shows that water returned to the test interval during the gas extraction phase.

iv. Circulation of water in the hydraulic lines and the interval for 10 minutes,

v. Repressurisation of the interval to 20.7 bar during 10 minutes,

vi. Compressibility test on the interval (value 6×10^{-9} Pa^{-1}).

Figure 39 shows the detailed measurements of gas pressure, with the sensor located in gas module PGZ1201PGZ01, then with the sensor connected to test interval PGZ1201PRE02.

Figure 39 Pressure measurements PGZ1201PRE02 and PGZ1201PGZ01 recorded on 5 May 2011 from midday to 8pm

The compressibility test showed that very little gas was dissolved in the interval. After 17 days of pressure recovery, a second compressibility test was performed on the 27 May 2011 (value of 4.1×10^{-9} Pa^{-1}). From this, it can be concluded that, during this period, there was no gas recovery into the interval's water.

An inflation test on packer PPK01 located below Interval 2 of PGZ1201 was performed on the 6 June 2011 to measure the interstitial pressure reaction in Interval 2. This test did not affect the pressure measurement in the interval, which was not the case during the compressibility test on 27 May, which induced an immediate "piston" effect on the packer (squeeze effect).

To better understand the behaviour of packers during this test, pressure sensors have been added to the packers, whose pressure was not previously monitored continuously:

- 6 June 2011: at the packer located at the bottom of the borehole with SAGD reference PGZ1201PPK03,
- 22 July 2011:
  - ✓ at the packer group surrounding Interval 3 of PGZ1201 (SAGD reference PGZ1201PPK04),
  - ✓ PGZ1202: all packers either side of Intervals 1 to 3. Here the SAGD reference sequence starts with PGZ1202PPK01 for the packer located at the end of the borehole and finishes with PGZ1202PPK04 for the packer group around Interval 3.

The act of adding these sensors produced a slight effect on the pressure measurements seen in Figure 30 and Figure 31.

The series of hydraulic tests (HYDRO2) was performed between 9 June and 30 June under fully stabilised hydraulic conditions. The test procedures were identical to those for HYDRO1 (a pulse-withdrawal test and a constant overpressure test).

Table 8 gives the results of HYDRO2. Both hydraulic tests were interpreted using a composite radial model with an inner and outer zone. We can see that hydraulic conductivity and specific storage are closed together (in the same range of uncertainty). This means that there is not any change after the gas injection (GAS1).

Table 8 Results of HYDRO2 and HYDRO1

Parameters		HYDRO1 (September 2009)	HYDRO2 (June 2011)
Hydraulic conductivity (m/s)	Inner zone	$6.4\ 10^{-11}$	$2.7\ 10^{-11}$
	Outer zone	$2.6\ 10^{-13}$	$2.0\ 10^{-13}$
Specific storage (1/m)	Inner zone	$1\ 10^{-6}$	$1\ 10^{-6}$
	Outer zone	$3\ 10^{-6}$	$2.7\ 10^{-6}$
Radius (m)		0.04	0.04

Finally, a series of compressibility tests on Intervals 1 to 3 of PGZ1202 and Intervals 1 and 3 of PGZ1201 were performed on 2 August 2011. The results of these tests are given in Table 9.

Table 9 Compressibility values for Intervals 1 and 3 of PGZ1201 and Intervals 1 to 3 of PGZ1202 measured on 2 August 2011

Intervals	Compressibility (10^{-9} Pa^{-1})
PGZ1201PRE01	1.71
PGZ1201PRE03	2.18
PGZ1202PRE01	1.64
PGZ1202PRE02	4.12
PGZ1202PRE03	2.1

The compressibility values show that there was little or no gas in these intervals. Only Interval 2 of PGZ1202 had a slightly higher value. It is hard to affirm that there was any gas in this interval.

On Interval 2 of PGZ1202 (Figure 31), sudden small reductions in pressure followed by return to equilibrium were observed from mid-May to early-July. This could indicate that gas travelled to this interval.

Without additional indication in favour of this, it is assumed that no gas travelled from the injection interval to Interval 2 of PGZ1202.

As an indication, the mass balance from filling with gas to refilling with water is given in Appendix 4. However, this mass balance is incomplete because the quantity of gas at the end of the extraction phase is not known, as the gas volume itself is not known.

8. Summary

8.1 Main results

The measurements obtained in the PGZ1 test validate the two-phase flow conceptual model.

8.1.1 Hydraulic tests and interference

Hydraulic tests performed at the beginning of the test in Interval 2 of PGZ1201 have been interpreted using a composite radial model. They give an estimate of the hydraulic conductivity of the rock of 2.6×10^{-13} m/s beyond a radius of 4 cm and a hydraulic conductivity of 6.4×10^{-11} m/s for the inner zone. The specific storage is considered uniform between the inner and outer zones.

During the constant pressure injection test, slight interference was detected in borehole PGZ1202. The effect has been satisfactorily reproduced using the same model. This result shows that a specific storage of between 1×10^{-6} m^{-1} and 3×10^{-6} m^{-1} applies in the undisturbed zone beyond 4cm from the borehole radius.

The monitoring of the period prior to the gas injection phase demonstrated the existence of drainage due to borehole PGZ1031. The permeability of the cement of this borehole is several orders of magnitude greater than the permeability of argillite. This drainage phenomena dampens over time as shown by the interstitial-pressure measurements after the gas injection phase (Figure 30 and Figure 31).

The pressure response to this drainage effect at the various monitoring intervals has been simulated using two approaches: one simplified (saturated flow with a constant pressure boundary) and one more complex (saturation at the draining borehole).

The hydraulic characteristics around the test, the test results and the interferences, confirm that the hydraulic conductivity of 2.6×10^{-13} m/s estimated at the decimetre scale is also valid at the metre scale. They also demonstrate that the description taken into account in the models used is valid for these test phases. Finally, they confirm the appropriateness of the specific storage (3×10^{-6} m^{-1}) used for the undamaged rock calculation.

8.1.2 Gas penetration into the argillite

Despite the fact that the pressure measurements were not corrected for this drainage effect, analysis of the GAS1 phase has shown that, after the third injection step (GRI3), the injection interval only contained gas (Figure 26). Thus, the pressure variation recorded after GRI3 represents gas invasion into the formation around the borehole wall. Conversely, before this third step, the pressure variation measured in the interval mainly corresponded to the expulsion of water from the interval into the rock.

This gas invasion from GRIS3 explains the sudden damping of interference observed in Interval 2 of PGZ1202 (see Figure 22), as the interference results from water flow around the injection chamber and the change in the behaviour of the packers around the test interval (see Section 7.2).

8.1.3 Gas entry pressure

A maximum value of 20 bar was obtained as the gas entry pressure into the rock, after having expelled all residual water initially in the interval. This value is small and, from the Young-Laplace equation, corresponds to a pore radius of 0.07 µm.

Given the existence of a 4-cm-thick EDZ around the borehole, **this maximal gas entry pressure clearly represents the entry pressure into the disturbed zone around the borehole.**

However, this discontinuity between the damaged zone and the undamaged zone is a simplification of the real situation. There is not a clear boundary with a specific radius around borehole PGZ1201 but rather a macroporosity that reduces with distance from the borehole wall until it reaches the same porosity distribution as that of the undamaged zone.

8.1.4 Gas invasion into the argillite

Figure 27, which represents pressure discrepancies at normalised injection step flowrates, and Figure 28, which gives the measured pressure variation during pressure recovery steps, show a very similar pattern.

Figure 40 was produced by combining data from Figure 27 and Figure 28. Their pressure variations as a function of time have been joined end to end. Overall, the pressure variation obtained seems very consistent.

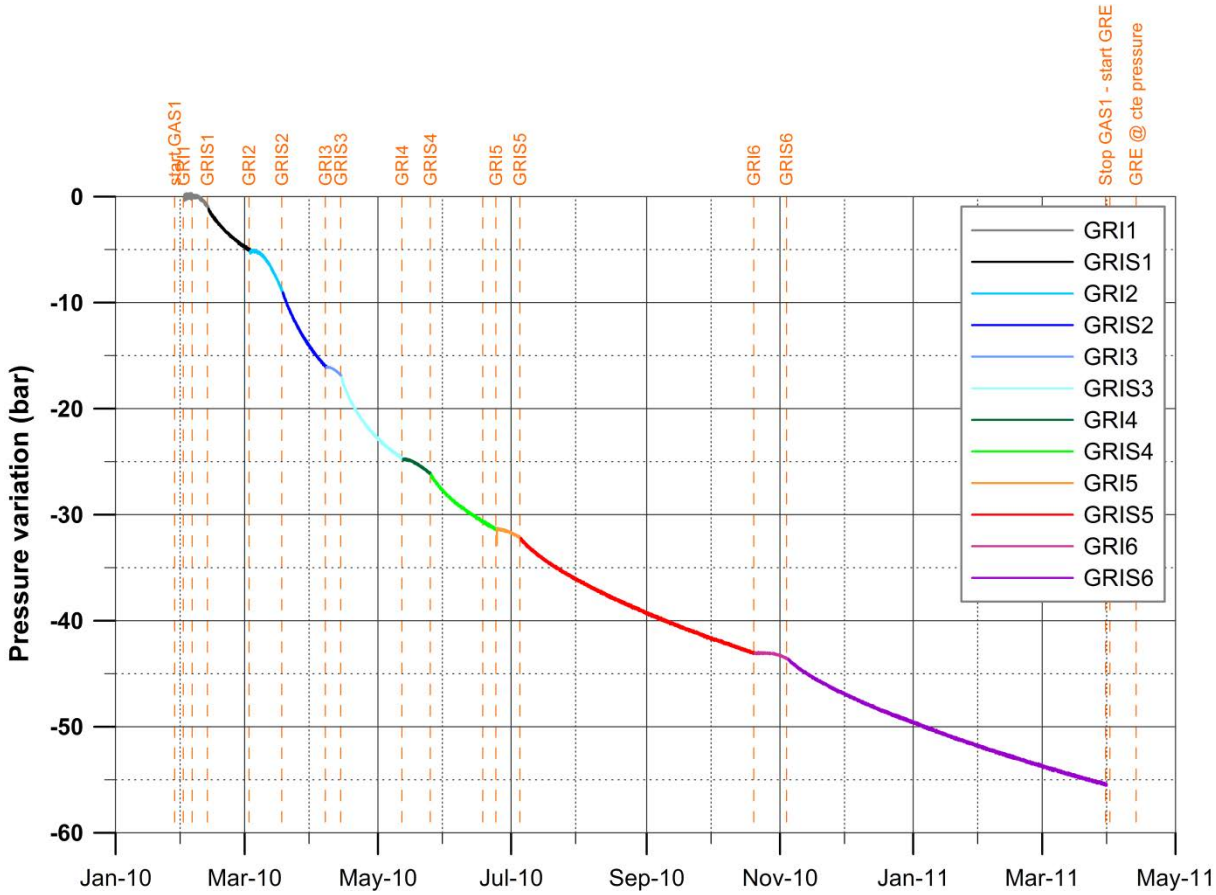

Figure 40 *Calculated pressure variation for all injection and pressure recovery steps*

It should be noted that this pressure variation describes the change over time of the variation in gas volume in the interval for normalised flowrate, eliminating the gas compressibility effect. When the interval is totally gas filled, i.e. from the end of GRI3, the pressure variation is damped. The flowrate of gas penetrating the formation reduces.

The slowing of gas penetration, which indicates a reduction in diffusivity, is probably due to an increase in the specific storage in the borehole's EDZ.

Indeed, from a hydraulics standpoint, the fact of injecting gas into the rock will change the saturation and, thus, the specific storage (see Section 7.2).

From this point of view, **the gas would remain mainly confined to the borehole's EDZ** and the slowing of the gas injection flowrate would signify that the gas is penetrating smaller and smaller pores as the pressure increases. With this in mind, analysis of the Horner plot (see Section 6.3.2) shows that the capillary pressure increases during the last three gas injection steps.

Even if gas has penetrated the undamaged rock, the quantities involved are small at this gas pressure.

8.1.5 Pathway dilation

No information that would demonstrate pathway dilation in the undamaged rock is available at this stage of the analysis.

8.2 Comparaison between HYDRO2 versus HYDRO1

Hydraulic tests give the same results despite the relatively long gas injection test (GAS1). Is what remains of the nitrogen gas in the argillite?

Appendix 1 Gas module

In the gas module, each flowmeter is associated with a control valve and this assembly is connected to a flowrate regulator which controls the gas flowrate either using pressure via a sensor or by directly acting on flowrate.

The three flowmeters installed in the gas module are thermal mass flowmeters from Brooks Instruments (sensor datasheets are given below).

The physics of the gas flowrate measurement is based on measuring heat transfer by the fluid itself. These devices are made of a thin-walled metal tube with heating resistors wound around the outside; fluid circulation causes loss of thermal equilibrium across the tube, which is proportional to the mass flowrate.

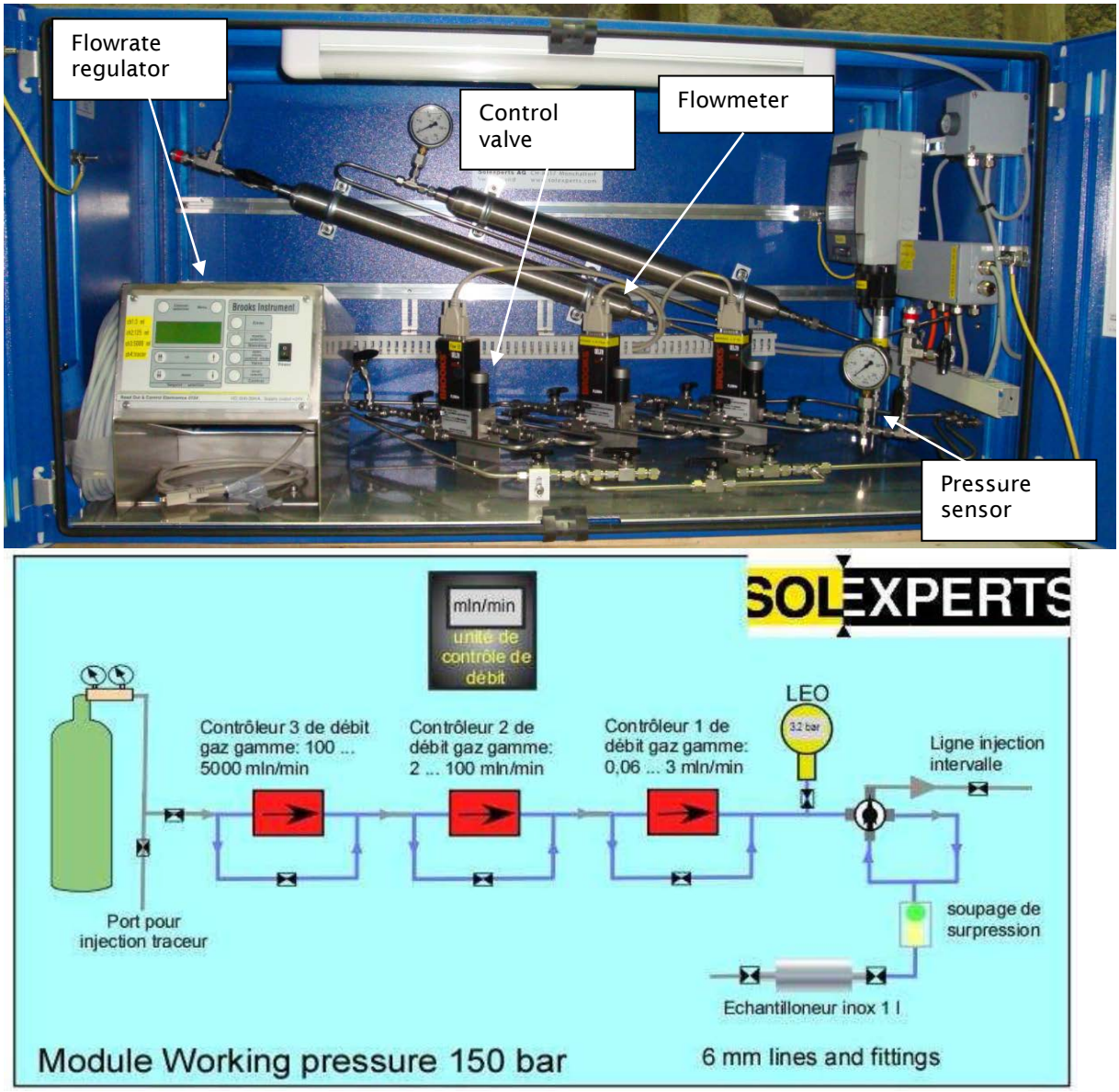

Figure 41 Photograph and schematic diagram of the gas module

Note that there is an uncertainty regarding the flowrate measurement provided by the flowmeter. As the flowmeter was calibrated for nitrogen (Appendix 2), water in the gas phase could invalidate the measurement in the extraction phase, as it depends on the specific heat capacity (at constant pressure) of the mixture.

Appendix 2 Sensor datasheets for the three gas flowmeters

PGZ1201DGZ01

Sensor type:	**Flowmeter**	
Manufactured by:	**Brooks**	
Technology:	**Thermal capacity based**	
Interface(N. of wires):	**2 wires (Signal, GND)**	
Model:	**SLA5850SH1AB1C2A1B2C6AA**	
Serial Number:	**T97577/013**	
Manufactured date:	**March 2009**	
Physical measurement:	**Flow**	*Unit:* **mln/min**
Dimensions:	**~ 15 x 15 cm**	
Weight:	**~ 500 g**	

Specifications:

Power	*230V extern*
Signal	*1..5 V*
Full scale	*0.06-3.00 mln/min*
Accuracy	*1 % of rate (20% - 100% FS)* *0.2% FS (below 20% FS)*
Repeatability	*0.2% of rate*

Product/Calibration Data Sheet

Device Information

Serial Number
T97577/013

Model Number
SLA5850SH1AB1C2A1B2C6AA

Customer
MERETEC

Customer Fluid
Nitrogen

Full Scale Flow
3 ml/min

Reference Temp/Pressure
0 °C/760 mmHg

Customer Inlet Pressure
100 bar g

Customer Outlet Pressure
0 - 95 bar g

Input
RS-485 4-20mA I/O (15 Pin D-Conn)

Output
RS-485 4-20mA I/O (15 Pin D-Conn)

Customer Part Number
N/A

Calibration Information

Calibration Inlet Pressure
100 bar g

Calibration Outlet Pressure
47.5 bar g

Gas Conversion Factor
1.000

Calibration Fluid
Nitrogen

Calibration Software/Revision
DeltaCal Version 1.3.28

Calibration Location
BMH

Calibration System ID
04015-02

Calibrator
BRH-op418

Calibration Date/Time
4/22/2009 3:55:48 PM

Calibration Procedure
CAL-060 Rev. 6

Calibration #
1 of 1

Mechanical Information

Valve Type
Normally Closed

Valve Seat Material
Viton

O-ring/Seal Material
Viton

Mounting Attitude
Horizontal

Power Supply
24 VDC

Reference Number
1

Alternate ID
N/A

Calibration Notes
Checked with customer conditions. (Hart Tag Name: 97577013, Hart Unique ID: 9757713, Hart Data Rate: 19200)

Calibration Check Data

Setpoint (%)	Output (%)	Flow (ml/min)	Error (% Rate)
0.00	0.032	0	-
5.00	0.470	0.14537	-3.09
10.00	10.054	0.29505	-1.65
25.00	24.992	0.74529	-0.63
50.00	49.933	1.49907	-0.06
75.00	75.053	2.24193	-0.36
100.00	100.085	2.99403	-0.20
0.00	-0.049	0	-

Setpoint Vs Error (% Rate) **0.7% Rate + 0.2% F.S.**

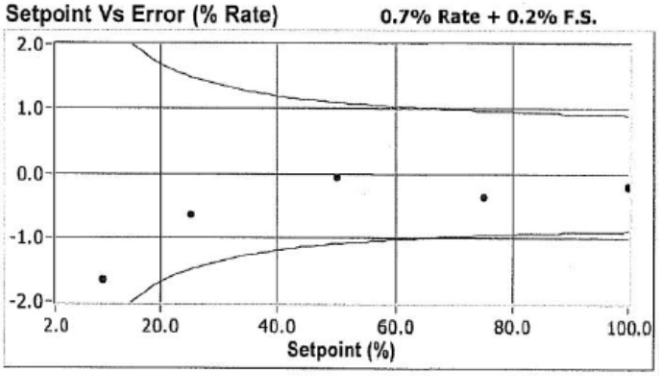

Brooks Instrument
407 West Vine Street
P.O. Box 903
Hatfield, PA 19440-0903 USA
T (215) 362-3700
F (215) 362-3745
www.BrooksInstrument.com

Brooks Instrument
Neonstraat 3
6718 WX Ede, Netherlands
T 31-318-549-300
F 31-318-549-309

Brooks Instrument Division
H-8000 Székesfehérvár
Berényi str 72-100, Hungary
T +36/22-543-775
F +36/22-543-778

Brooks Instrument
1-4-4 Kitasuna Koto-Ku
Tokyo, 136-0073 Japan
T 81-3-5633-7106
F 81-3-5633-7124

BROOKS® INSTRUMENT

Approved by: _____

This report shall not be reproduced, except in full, without written approval from Brooks Instrument

Ref. OPN-004-1

Page 1 of 1

PGZ1201DGZ02

Sensor type:	**Flowmeter**	
Manufactured by:	**Brooks**	
Technology:	**Thermal capacity based**	
Interface(N. of wires):	**2 wires (Signal, GND)**	
Model:	**SLA5850SH1AB4C2A1B3M5AA**	
Serial Number:	**T97577/016**	
Manufactured date:	**May 2009**	
Physical measurement:	**Flow**	*Unit:* **mln/min**
Dimensions:	**~ 15 x 15 cm**	
Weight:	**~ 500 g**	

Specifications:

Power	*230V extern*
Signal	*1..5 V*
Full scale	*2.5-125 mln/min*
Accuracy	*1 % of rate (20% - 100% FS)* *0.2% FS (below 20% FS)*
Repeatability	*0.2% of rate*

Product/Calibration Data Sheet

Device Information

Serial Number
T97577/016

Model Number
SLA5850SH1AB4C2A1B3M5AA

Customer
MERETEC

Customer Fluid
Nitrogen

Full Scale Flow
125 ml/min

Reference Temp/Pressure
0 °C/760 mmHg

Customer Inlet Pressure
200 bar g

Customer Outlet Pressure
0 - 195 bar g

Input
RS-485 4-20mA I/O (15 Pin D-Conn)

Output
RS-485 4-20mA I/O (15 Pin D-Conn)

Customer Part Number
N/A

Calibration Information

Calibration Inlet Pressure
100 bar g

Calibration Outlet Pressure
0 bar g

Gas Conversion Factor
1.000

Calibration Fluid
Nitrogen

Calibration Software/Revision
DeltaCal Version 1.3.28

Calibration Location
BMH

Calibration System ID
04016/02

Calibrator
BRH-op418

Calibration Date/Time
5/26/2009 12:53:02 PM

Calibration Procedure
CAL-060 Rev. 6

Calibration #
1 of 1

Mechanical Information

Valve Type
Normally Closed - High Pressure

Valve Seat Material
Viton

O-ring/Seal Material
Viton

Mounting Attitude
Horizontal

Power Supply
24 VDC

Reference Number
1

Alternate ID
N/A

Calibration Notes
Checked with variable outlet pressure. (Hart Tag Name: 97577016, Hart Unique ID: 9757716, Hart Data Rate: 19200)

Calibration Check Data

Setpoint (%)	Output (%)	Flow (ml/min)	Error (% Rate)
0.00	-0.032	0	-
5.00	5.106	6.14747	-1.64
10.00	10.014	12.27079	-1.83
25.00	25.015	31.46002	0.67
50.00	50.033	62.16617	-0.53
75.00	75.006	94.0991	0.37
100.00	100.011	124.85987	-0.11
0.00	-0.055	0	-

Setpoint Vs Error (% Rate) **0.7% Rate + 0.2% F.S.**

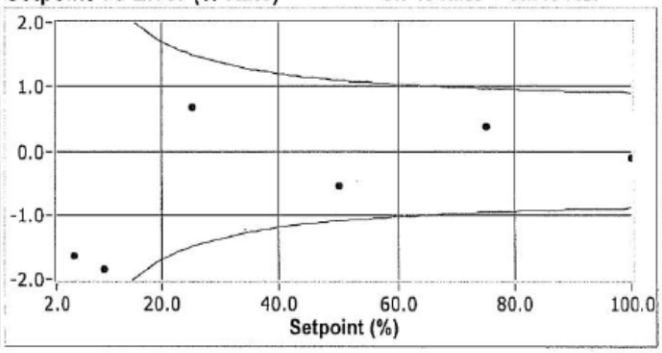

Brooks Instrument
407 West Vine Street
P.O. Box 903
Hatfield, PA 19440-0903 USA
T (215) 362-3700
F (215) 362-3745
www.BrooksInstrument.com

Brooks Instrument
Neonstraat 3
6718 WX Ede, Netherlands
T 31-318-549-300
F 31-318-549-309

Brooks Instrument Division
H-8000 Székesfehérvár
Berényi str 72-100, Hungary
T +36/22-543-775
F +36/22-543-778

Brooks Instrument
1-4-4 Kitasuna Koto-Ku
Tokyo, 136-0073 Japan
T 81-3-5633-7106
F 81-3-5633-7124

BROOKS® INSTRUMENT

Approved by: _____

This report shall not be reproduced, except in full, without written approval from Brooks Instrument

Ref. OPN-004-1

Page 1 of 1

PGZ1201DGZ03

Sensor type:	**Flowmeter**	
Manufactured by:	**Brooks**	
Technology:	**Thermal capacity based**	
Interface(N. of wires):	**2 wires (Signal, GND)**	
Model:	**SLA5850SE1AB4C2A1W4Y5AA**	
Serial Number:	**T97577/019**	
Manufactured date:	**March 2009**	
Physical measurement:	**Flow**	*Unit:* **mln/min**
Dimensions:	**~ 15 x 15 cm**	
Weight:	**~ 500 g**	

Specifications:

Power	*230V extern*
Signal	*1..5 V*
Full scale	*100-5000 mln/min*
Accuracy	*1 % of rate (20% - 100% FS)* *0.2% FS (below 20% FS)*
Repeatability	*0.2% of rate*

Product/Calibration Data Sheet

Device Information

Serial Number
T97577019

Model Number
SLA5850S1HAB1G2A1W4Y5AA

Customer
MERETEC AG

Customer Fluid
Nitrogen

Full Scale Flow
5000 sccm

Reference Temp/Pressure
0 °C/760 mmHg

Customer Inlet Pressure
200 bar g

Customer Outlet Pressure
195 bar g

Input
RS-485 4-20mA I/O (PG11 Cable Gland)

Output
RS-485 4-20mA I/O (PG11 Cable Gland)

Customer Part Number
N/A

Calibration Information

Calibration Inlet Pressure
200 bar g

Calibration Outlet Pressure
195 bar g

Gas Conversion Factor
1.000

Calibration Fluid
Nitrogen

Calibration Software/Revision
DeltaCal Version 1.3.28

Calibration Location
Ede

Calibration System ID
04000-04

Calibrator
OP-73

Calibration Date/Time
6/30/2009 3:50:25 PM

Calibration Procedure
CAL-060 Rev. 6

Calibration #
1 of 1

Mechanical Information

Valve Type
Normally Closed

Valve Seat Material
Viton

O-ring/Seal Material
Viton

Mounting Attitude
Horizontal

Power Supply
24 VDC

Reference Number
1

Alternate ID
N/A

Calibration Notes
N/A (Hart Tag Name: 97577019, Hart Unique ID: 9757719, Hart Data Rate: 19200)

Calibration Check Data

Setpoint (%)	Output (%)	Flow (sccm)	Error (% Rate)
0.00	0.064	0	-
5.00	4.953	251.91724	0.77
10.00	9.949	502.44617	0.49
25.00	24.982	1256.66245	0.53
50.00	50.008	2509.355	0.37
75.00	75.008	3749.67739	-0.01
100.00	100.229	5001.04299	0.02
0.00	-0.037	0	-

Setpoint Vs Error (% Rate)

1% Rate, 0.2% F.S. < 20%

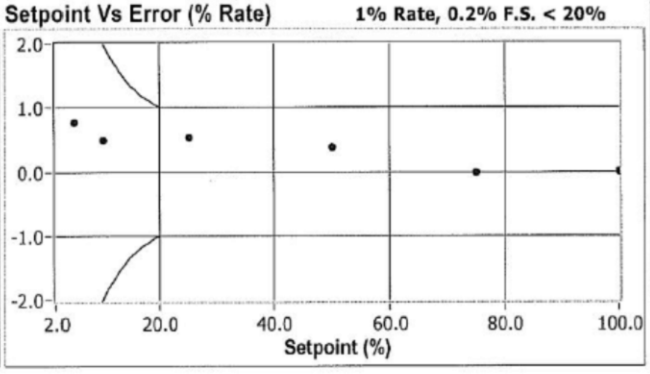

Brooks Instrument
407 West Vine Street
P.O. Box 903
Hatfield, PA 19440-0903 USA
T (215) 362-3700
F (215) 362-3745
www.BrooksInstrument.com

Brooks Instrument
Neonstraat 3
6718 WX Ede, Netherlands
T 31-318-549-300
F 31-318-549-309

Brooks Instrument Division
H-8000 Székesfehérvár
Berényi str 72-100, Hungary
T +36/22-543-775
F +36/22-543-778

Brooks Instrument
1-4-4 Kitasuna Koto-Ku
Tokyo, 136-0073 Japan
T 81-3-5633-7105
F 81-3-5633-7124

BROOKS® INSTRUMENT

Approved by: _____

This report shall not be reproduced, except in full, without written approval from Brooks Instrument

Ref. OPN-004-1

Page 1 of 1

Appendix 3 Volume for the gas module and extraction system

Système injection	L (m)	ID (mm)	Vol (cm3)	
Module : lignes de "gros débitmètre" à "moyen débitmètre"	1.05	4	13	
Module : lignes de "moyen débitmètre" à "petit débitmètre"	1.05	4	13	
Module : lignes de "petit débitmètre" à "fin module"	0.8	4	10	
Ligne Module vers "Panneau de contrôle"	3.05	2.4	14	
Total : Volume système d'injection entre débitmètre et "Panneau de contrôle"				
Cas 1 : injection par gros débitmètre			**50**	cm3
Cas 2 : injection par moyen débitmètre			**37**	cm3
Cas 3 : injection par petit débitmètre			**24**	cm3

Injection system	L (m)	ID (mm)	Vol (cm^3)
Module: “large flowmeter” to “medium flowmeter” lines	1.05	4	13
Module: “medium flowmeter” to “small flowmeter” lines	1.05	4	13
Module: “small flowmeter” to “module end” lines	0.8	4	10
Module to “Control Panel” line	3.05	2.4	14
Total: Injection system volume between flowmeter and “Control Panel”			
Case 1: Large flowmeter injection			50 cm^3
Case 2: Medium flowmeter injection			37 cm^3
Case 3: Small flowmeter injection			24 cm^3

Système extraction	L (m)	ID (mm)	Vol (cm3)	
Ligne "panneau de contrôle" vers "gros T"	8.4	2.4	38	
Gros T			51	
Colonne WCFM	1.05	10	82	
Ligne "gros T" vers caisson	3.25	2.4	15	
Caisson			3870	
Ligne caisson vers "T sur ligne gaz WCFM"	1.4	2.4	6	
Ligne gaz WCFM	1.15	3	8	
Ligne "T sur ligne gaz WCFM" vers Module	6.7	2.4	30	
Module : lignes de "début module" à "gros débitmètre"	1.3	4	16	
Module : lignes de "gros débitmètre" à "moyen débitmètre"	1.05	4	13	
Module : lignes de "moyen débitmètre" à "petit débitmètre"	1.05	4	13	
Total : Volume système d'extraction entre "Panneau de contrôle" et débitmètre				
Cas 1 : extraction par gros débitmètre			**4117**	cm3
Cas 2 : extraction par moyen débitmètre			**4130**	cm3
Cas 3 : extraction par petit débitmètre			**4144**	cm3

Appendix 4 Mass balance

The mass balance between the injection and extraction phases is given in Table 10. Nitrogen dissolution and diffusion are neglected:

Table 10 Mass balance between gas injection and extraction

In moles	Injection	Extraction	Storage
Filling with gas (volume of 1040 cm³ and pressure of 39.6 bar)			1.68
Injection at constant pressure	0.09		
GRI1	0.53		
GRI2	0.98		
GRI3	1.34		
GRI4	1.24		
GRI5	0.89		
GRI6	1.28		
Addition of the extraction system (volume of 4114 cm³ and pressure of 79 bar)			13.32
GRE (gas extraction)		13.2	
Quantity remaining in the extraction system (volume of 4114 cm³ and pressure of 20.6 bar)			3.47

After the gas extraction phase and before the final purge of the gas injection interval, the balance is as follows:

- Quantity of nitrogen injected: 6.35 moles
- Quantity of nitrogen extracted: 13.2 moles
- Variation in nitrogen storage: 1.68 + 13.32 – 3.47 = 11.53 moles

The quantity of nitrogen remaining in the interval is: 6.35 + 11.53 – 13.2 = 4.68 moles.

It is not possible to calculate the quantity of gas extracted during the final purge as the gas volume is not known.

9. Glossary

SAGD French acronym for data acquisition and management system

10. References

MARSCHALL P., HORSEMAN S. AND GIMMI T., OIL & GAS SCIENCE AND TECHNOLOGY – REV. IFP, VOL. 60 (2005), NO. 1, PP. 121-139
FREEZE R.A. AND CHERRY J.A. 1979: GROUNDWATER, PRENTICE-HALL INTERNATIONAL (UK), LONDON, ISBN 0-13- 365312-9
SCHANZ, T., 2003, UNSATURATED SOILS: NUMERICAL AND THEORETICAL APPROACHES, PROCEEDING OF THE INTERNATIONAL CONFERENCE "FROM EXPERIMENTAL EVIDENCE TOWARDS NUMERICAL MODELLING OF UNSATURATED SOILS", WEIMAR, GERMANY, SEPTEMBER 18-19, 2003

The documents listed below are ANDRA documents associated with test PGZ1 or cited in the text.

Andra's reference	Issued by	Title
D.RP.0GOL.05.001	GOLDER ASSOCIATES	Gas threshold pressure test – interpretation report – borehole EST363.
D.NT.0CPE.08.022	AF CONSULT - INTERA	"*Dimensionnement des tests au gaz pour la caractérisation de la formation saine. Proposition technique*" (Design of gas tests for characterising the undisturbed formation. Technical proposal).
D.RP.0CPE.09.002	AF CONSULT - INTERA	"*Tests au gaz pour la caractérisation de la formation saine – Rapport Préliminaire*" (Gas tests for characterising the undisturbed formation - Preliminary Report).
D.RP.0CPE.09.009	AF CONSULT - SOLEXPERTS	"*Expérimentation OHZ / Optimisation des contraintes pour l'analyse des tests hydrogéologiques*" (OHZ experiment / Optimisation of constraints for the analysis of hydrogeology tests).
D.RP.0CPE.09.0028	AF CONSULT - SOLEXPERTS	"*Tests hydrauliques dans le forage de l'unité de programme PGZ1 de la galerie GED - Forages PGZ1201 et PGZ1202*" (Hydraulic tests in the boreholes of the PGZ1 Programme Unit in the GED drift – Boreholes PGZ1201 and PGZ1202).
D.RP.0CPE.09.008	AF CONSULT - SOLEXPERTS	"*Tests hydrauliques dans les forages de l'unité de programme GED (PGZ1, TED, OHZ, SDZ) – Rapport Préliminaire*" (Hydraulic tests in the GED Unit Programme boreholes (PGZ1, TED, OHZ, SDZ) – Preliminary Report).
D.RP.0CPE.09.017	AF CONSULT - SOLEXPERTS	"*Instrumentation de mesures extensométriques – essai de caractérisation de la formation saine PGZ1 - Forage PGZ1031 - Rapport d'Installation et de Mesure initiales (RIM)*" (Instrumentation for extensometer measurements – test for characterising the undisturbed PGZ1 formation – Borehole PGZ1031—Installation and Initial Measurements Report).

D.RP.0CPE.09.020	AF CONSULT - SOLEXPERTS	"*Tests hydrauliques dans le forage d'injection de l'unité de programme PGZ1 en galerie GED - Forages PGZ1201*" (Hydraulic tests in the injection borehole of the PGZ1 Programme Unit in the GED drift – Borehole PGZ1201).
D.RP.0CPE.10.0006	AF CONSULT - INTERA	"*Palier d'injection GRI1 dans l'essai de caractérisation de la formation saine. Forage d'injection PGZ1201*" (Injection step GRI1 in the undisturbed formation characterisation test. Injection borehole PGZ1201).
D.RP.0CPE.10.0008	AF CONSULT - INTERA	"*Palier d'injection GRI2 dans l'essai de caractérisation de la formation saine. Forage d'injection PGZ1201.*" (Injection step GRI2 in the undisturbed formation characterisation test. Injection borehole PGZ1201).
D.RP.0CPE.10.0015	AF CONSULT - INTERA	"*Palier d'injection GRI3 dans l'essai de caractérisation de la formation saine. Forage d'injection PGZ1201*" (Injection step GRI3 in the undisturbed formation characterisation test. Injection borehole PGZ1201).
D.RP.0CPE.10.0019	AF CONSULT - INTERA	"*Palier d'injection GRI4 dans l'essai de caractérisation de la formation saine. Forage d'injection PGZ1201*" (Injection step GRI4 in the undisturbed formation characterisation test. Injection borehole PGZ1201).
D.RP.0CPE.10.0025	AF CONSULT - INTERA	"*Palier d'injection GRI5 dans l'essai de caractérisation de la formation saine. Forage d'injection PGZ1201*" (Injection step GRI5 in the undisturbed formation characterisation test. Injection borehole PGZ1201).
D.RP.0CPE.10.0037	AF CONSULT - INTERA	"*Paliers d'injection de gaz GRI1 à GRI5 à PGZ1201*" (Gas injection steps GRI1 to GRI5 in PGZ1201).
D.RP.0CPE.11.0001	AF CONSULT	"*Analyse de l'impact hydraulique du forage PGZ1031 sur les pressions mesurées au forage PGZ1201 et PGZ1202*" (Analysis of the hydraulic impact of borehole PGZ1031 on the pressures measured in boreholes PGZ1201 and PGZ1202).
D.RP.0CPE.11.0003	AF CONSULT - INTERA	"*Palier d'injection GRI6 dans l'essai de caractérisation de la formation saine. Forage d'injection PGZ1201*" (Injection step GRI6 in the undisturbed formation characterisation test. Injection borehole PGZ1201).
D.RP.0CPE.11.0004	AF CONSULT – INTERA - SOLEXPERTS	"*Expérimentation PGZ1 - PGZ1201 transition GAS1-HYDRO2 – Extraction de gaz & Abaissement de la pression*" (PGZ1 experiment – PGZ1201 GAS1-HYDRO2 transition – Gas extraction and pressure reduction).